



Self-consistent random-phase approximation based on the relativistic Hartree-Fock theory: Role of ρ -tensor coupling

Zhiheng Wang (王之恒),^{1,2,3,4} Tomoya Naito (内藤智也) ^{5,4}
Haozhao Liang (梁豪兆),^{4,5,*} and Wen Hui Long (龙文辉) ^{1,2,†}

¹*School of Nuclear Science and Technology, Lanzhou University, Lanzhou 730000, China*

²*Joint Department for Nuclear Physics, Lanzhou University and Institute of Modern Physics, Chinese Academy of Sciences, Lanzhou 730000, China*

³*Faculty of Pure and Applied Sciences, University of Tsukuba, Tsukuba 305-8571, Japan*

⁴*RIKEN Nishina Center, Wako 351-0198, Japan*

⁵*Department of Physics, Graduate School of Science, The University of Tokyo, Tokyo 113-0033, Japan*



(Received 14 January 2020; revised manuscript received 10 March 2020; accepted 13 April 2020; published 12 June 2020)

The framework of the random-phase approximation (RPA) based on the relativistic Hartree-Fock (RHF) theory is extended to achieve a self-consistent calculation with the ρ -meson tensor coupling. The model self-consistency is verified by the check of the isobaric analog state, and it is found that the ρ -tensor and ρ -vector-tensor couplings play significant roles in maintaining the self-consistency. Using the RHF Lagrangian PKA1, the properties of the Gamow-Teller resonances (GTR) are investigated, in which the roles played by the particle-hole residual interaction of various meson-nucleon couplings are clarified in details. Furthermore, the effects of the tensor force, which is introduced naturally via the Fock terms, are analyzed by comparing the calculations with full Lagrangians and the ones artificially dropping the tensor force components. It is found that for the RHF Lagrangians PKO*i* ($i = 1, 2, 3$) and PKA1, the tensor forces play the role mainly via the RHF mean field rather than via the RPA residual interaction in determining the GTR. Moreover, the tensor-force effects are not as strong as those indicated by the Skyrme Hartree-Fock calculations.

DOI: [10.1103/PhysRevC.101.064306](https://doi.org/10.1103/PhysRevC.101.064306)

I. INTRODUCTION

The nuclear isospin excitations [1,2] refer to the transitions from the ground state of a nucleus (N, Z) to the final states in its neighboring nuclei ($N \mp 1, Z \pm 1$), where the upper and lower signs correspond to the isospin lowering T_- and raising T_+ channels, respectively. These excitations can take place spontaneously for instance in the β^\pm decays, or be triggered by external interactions, like the charge-exchange reactions (p, n), ($^3\text{He}, t$), etc. In these excitation modes, the spin-up and spin-down nucleons can oscillate in phase or out of phase, and the latter are usually referred as the spin-flip transitions or the spin-isospin excitations.

Nowadays, it is well recognized that the spin-isospin excitations are significant not only in nuclear physics but also in astrophysics, particle physics, etc. For example, the neutron-skin thickness, an important quantity in nuclear structure but difficult to be measured [3], can be extracted indirectly from the properties of spin-isospin excitations [4–6]. For astrophysics, the spin-isospin excitations can provide essential inputs for exploring the origin of heavy elements [7–21]. One

of the well-known examples is the low-energy Gamow-Teller resonance (GTR), which determines the β -decay half-lives of hundreds of neutron-rich nuclei located on the rapid neutron capture process (r -process) path of stellar nucleosynthesis. Besides, the unitarity of the Cabibbo-Kobayashi-Maskawa matrix [22,23] can be tested through the isospin corrections deduced from the isobaric analogy states (IAS) in the super-allowed Fermi β decays [24–27]. In this work, our particular interests are partly devoted to the spin and isospin information of the nuclear interactions in the medium carried by the spin-isospin excitations [28].

In nuclear physics, it is a longstanding open problem to understand the nuclear interactions in the medium, which are usually referred as the effective nuclear interactions. As a typical example, the important ingredient of nuclear force—the tensor force has received tremendous attention [29] over the past years, accompanying the development of the modern radioactive ion beam facilities and detectors [30–35]. Nowadays, it is well recognized that the tensor force should be considered as an essential ingredient of the effective interactions. Nevertheless, there still remain an amount of open questions, e.g., the uncertainty of the strengths of the tensor force in the effective interactions, seeing the recent review [36] and references therein. To pin down the properties of the tensor force, it would be quite helpful to find appropriate observables which are sensitive to the tensor force while they

*haozhao.liang@riken.jp

†longwh@lzu.edu.cn

do not essentially depend on the other ingredients of nuclear force [36–40]. Notice the fact mentioned above that the spin-isospin excitations carry rich spin and isospin information of the effective interactions. Thus, being consistent with the spin-dependent nature of the tensor force [29], one would naturally expect some valuable information extracted from the spin-isospin excitations, which may pave an efficient way to constrain the strength of the tensor force [41].

The density functional theory (DFT) [42–44], which reduces the many-body problems formulated in terms of N -body wave functions to the one-body level with local density distributions, has achieved great successes in the description of not only the ground-state but also the excited properties for almost all the nuclides on the whole nuclear chart [45]. Within the framework of the nonrelativistic nuclear DFT, the effects of the tensor force on the spin-isospin excitations have been intensively investigated by the random-phase approximation (RPA) based on the Skyrme Hartree-Fock (Skyrme HF) theory [41,46–48], and the corresponding constraints on the strength of tensor force have also been explored [38]. In the Skyrme HF theory, the tensor forces were added on top of existing parameter sets and fitted perturbatively [49,50], or refitted with an equal footing as other central components [51,52]. It shall be noticed that in both cases additional adjustable parameters associated with the tensor force are introduced, which still cannot be well constrained yet [36,38].

On the contrary, within the relativistic version of nuclear DFT, also known as the covariant DFT (CDFT) [45,53–58], the tensor forces can arise naturally with the implement of the Fock terms of the meson-nucleon couplings [59–65]. Thus, under the CDFT with the Fock terms, namely the relativistic Hartree-Fock (RHF) theory [59–61,66–68], the strengths of the tensor forces are determined by the intrinsic meson-nucleon coupling strengths, other than introducing extra free parameters. This may serve as a distinctive advantage of CDFT for the efficient constraint of the effective tensor force. It shall be mentioned that within the relativistic mean-field (RMF) theory, a popular branch of the CDFT containing only the Hartree terms of the meson-nucleon couplings, the tensor force components are missing due to the limitation of the Hartree approach.

In fact, with the explicit treatment of the Fock terms, significant improvements have been obtained by the RHF theory in the self-consistent description of shell evolution [62,63,69,70], nuclear spin-isospin excitations [17,26,71–73], nuclear effective masses [60], symmetry energy [74–78], new magicity [70,79], the origin of pseudospin symmetry [80,81], etc. Moreover, considering the ρ -tensor (ρ -T) coupling that plays the role almost fully via the Fock terms, the spurious shell closures $N(Z) = 58$ and 92, which are commonly found in the RMF calculations and the one with the RHF Lagrangians PKO i ($i = 1, 2, 3$), are eliminated eventually by the RHF Lagrangian PKA1 [61] with appropriate restoration of the pseudospin symmetry for the high- j pseudospin partners [81,82]. Even though, one shall notice that the tensor force components, introduced naturally by the Fock terms, are mixed with the other components indeed, like the central ones in the relevant meson-nucleon couplings. This made the

quantitative analyses of the tensor-force effects in determining the spin-isospin excitations inaccessible before, although the fully self-consistent RPA method based on the RHF theory [71] has already been established.

With the self-consistent RPA method based on the RHF theory (denoting as RHF + RPA hereafter), the properties of GTR and spin-dipole resonances (SDR) in doubly magic nuclei can be well described without introducing any extra free parameters into the particle-hole (ph) residual interaction [71,72,83]. Specifically, the coefficient of the zero-range pionic counter-term remains its physical value $g'_\pi = 1/3$, while it is treated as a free parameter to reproduce the GTR energies for the RPA method based on RMF theory, namely $g'_\pi \approx 0.6$. Afterwards, the self-consistent quasi-particle random phase approximation (QRPA) [17] was established based on the relativistic Hartree-Fock-Bogoliubov (RHFB) theory [68], namely the RHFB + QRPA method, which achieves many successes not only in describing the properties of IAS and GTR, but also in reproducing the β -decay half-lives of the open-shell nuclei on the nuclear chart [17,73]. Notice that the mentioned studies were performed with the RHF Lagrangians PKO i , in which the degree of freedom associated with the ρ -T coupling is not taken into account. As mentioned above, the RHF Lagrangian PKA1 that contains the ρ -T coupling has brought notable improvement in describing the single-particle structure properties of nuclei. Since the ρ -T coupling is also one of the essential origins of the tensor force [61,62,84], it is quite expectable to extend the existing RHF + RPA method by considering the degree of freedom of the ρ -T coupling, as well as the accompanying ρ -vector-tensor (ρ -VT) coupling [61].

Very recently, the tensor force components, introduced naturally by the Fock terms of various meson-nucleon coupling channels, have been identified quantitatively via the nonrelativistic reduction [85], which indeed paves an efficient way to study the tensor-force effects on the spin-isospin excitations within the RHF + RPA method. Specifically on the tensor-force effects, this also makes the direct comparison possible between the CDFT and nonrelativistic DFT. Aiming at that, we first extend the RHF + RPA method by including the ρ -T and ρ -VT couplings in the particle-hole residual interaction. Further, the properties of GTR are explored by employing the RHF Lagrangian PKA1, and particular efforts are devoted on the roles of the ρ -T and ρ -VT couplings. Moreover, to quantify the tensor-force effects on the GTR, the effects of the tensor force in both RHF mean field and RPA ph residual interactions are analyzed in details with the technology proposed in Ref. [85].

This paper is organized as follows. In Sec. II, the general formalism of the RHF + RPA method is briefly introduced, and the method to evaluate the contribution tensor force in the RPA ph residual interactions is given in details. The discussion on the properties of IAS and GTR as well as the tensor-force effects on GTR are given in Sec. III. Summary and perspectives are given in Sec. IV.

II. THEORETICAL FRAMEWORK

In this section, we will at first introduce the basic ideas of RHF approach briefly and then illustrate the framework

of RHF + RPA. The formula to extract the contribution of tensor force in the RPA ph residual interactions will also be presented in details.

A. Relativistic Hartree-Fock theory

In the relativistic framework, the nucleus is described as a system of Dirac nucleons that interact through the exchange of massive mesons [84,86,87]. Coincident with such a picture, an effective Lagrangian density \mathcal{L} , the starting point of the RHF theory, can be constructed by considering the degrees of freedom associated with the nucleon field ψ , two isoscalar meson fields σ and ω , two isovector meson fields π and ρ , and the photon field A . More precisely, it may contain the free parts of the nucleon, meson, and photon fields, and the interaction parts between nucleons and mesons (photons) [59–61], respectively, \mathcal{L}_0 and \mathcal{L}_1 ,

$$\mathcal{L} = \mathcal{L}_0 + \mathcal{L}_1, \quad (1)$$

where

$$\begin{aligned} \mathcal{L}_0 = & \bar{\psi}(i\gamma_\mu\partial^\mu - M)\psi + \frac{1}{2}\partial_\mu\sigma\partial^\mu\sigma - \frac{1}{2}m_\sigma^2\sigma^2 - \frac{1}{4}\Omega_{\mu\nu}\Omega^{\mu\nu} \\ & + \frac{1}{2}m_\omega^2\omega_\mu\omega^\mu - \frac{1}{4}\vec{R}_{\mu\nu}\cdot\vec{R}^{\mu\nu} + \frac{1}{2}m_\rho^2\vec{\rho}_\mu\cdot\vec{\rho}^\mu \\ & + \frac{1}{2}\partial_\mu\vec{\pi}\cdot\partial^\mu\vec{\pi} - \frac{1}{2}m_\pi^2\vec{\pi}\cdot\vec{\pi} - \frac{1}{4}F_{\mu\nu}F^{\mu\nu}, \end{aligned} \quad (2a)$$

$$\begin{aligned} \mathcal{L}_1 = & -\bar{\psi}\left[g_\sigma\sigma + g_\omega\gamma^\mu\omega_\mu + g_\rho\gamma^\mu\vec{\tau}\cdot\vec{\rho}_\mu - \frac{f_\rho}{2M}\sigma^{\mu\nu}\vec{\tau}\cdot\partial_\nu\vec{\rho}_\mu\right. \\ & \left.+ \frac{f_\pi}{m_\pi}\gamma_5\gamma^\mu\vec{\tau}\cdot\partial_\mu\vec{\pi} + e\gamma^\mu\frac{1-\tau_3}{2}A_\mu\right]\psi, \end{aligned} \quad (2b)$$

with the field tensors $\Omega^{\mu\nu} \equiv \partial^\mu\omega^\nu - \partial^\nu\omega^\mu$, $\vec{R}^{\mu\nu} \equiv \partial^\mu\vec{\rho}^\nu - \partial^\nu\vec{\rho}^\mu$, and $F^{\mu\nu} \equiv \partial^\mu A^\nu - \partial^\nu A^\mu$. In the above expressions, M and m_ϕ ($\phi = \sigma, \omega, \rho, \pi$) denote the masses of nucleon and mesons, respectively, and g_ϕ ($\phi = \sigma, \omega, \rho$) and $f_{\phi'}$ ($\phi' = \rho, \pi$) represent the meson-nucleon coupling strengths. In this paper, the isovectors are denoted by arrows and the space vectors are in bold type. In the interaction Lagrangian density \mathcal{L}_1 Eq. (2b), we consider the Lorentz σ -scalar (σ -S), ω -vector (ω -V), ρ -vector (ρ -V), ρ -tensor (ρ -T), π -pseudovector (π -PV), and photon-vector (A -V) couplings. It is worthwhile to mention that the contributions of ρ -T coupling, as well as the accompanying ρ -vector-tensor (ρ -VT) one, are taken into account in the RPA residual interactions for the first time. To avoid confusion, the capital letter ‘‘T’’ represents the *Lorentz tensor* coupling, and the lower case ‘‘t’’ will be used later to denote the *tensor* force.

Within the RHF theory, the total energy of the system can be derived as the expectation value of the Hamiltonian \hat{H} [68] on the trial Hartree-Fock ground state $|\Phi\rangle$, i.e.,

$$\begin{aligned} E = \langle\Phi|\hat{H}|\Phi\rangle = & \sum_a \langle a|\hat{T}|a\rangle \\ & + \frac{1}{2} \sum_{ab} [\langle ab|\hat{V}(1,2)|ab\rangle - \langle ab|\hat{V}(1,2)|ba\rangle], \end{aligned} \quad (3)$$

where the sum over a and b run over all the occupied single-particle states in the Fermi sea, corresponding to the

so-called no-sea approximation [87], and the operators \hat{T} and $\hat{V}(1,2)$ represent the single-particle kinetic energy and two-body interaction, respectively. The variation of the energy E with respect to the single-particle states leads to the Hartree-Fock equation, namely the integro-differential Dirac equation [59,68,80,88].

The two-body interaction provided by each meson-nucleon coupling is formally represented as

$$\hat{V}_\phi(1,2) = g_\phi(1)g_\phi(2)I_\phi(1,2), \quad (4)$$

where ϕ denotes various meson-nucleon coupling channels, i.e., $\phi = \sigma$ -S, ω -V, ρ -V, ρ -VT, ρ -T, π -PV, and A -V, and g_ϕ represents the coupling strengths. The expressions of \hat{V}_ϕ are shown explicitly in Appendix A. Note that the coupling strengths are taken as functions of the baryon density in the density-dependent RHF theory. More details about the RHF theory are referred to Refs. [59–61,74,85,88].

B. Random-phase approximation

1. RPA equations in general form

The relativistic RPA equation is known to be equivalent to the time-dependent relativistic Hartree(-Fock) equation in the small amplitude limit, only if the ph configurations include not only the pairs formed from the occupied and unoccupied Fermi states but also those formed from the occupied Fermi states and empty Dirac states [89]. In this paper, the RPA equation will be derived via the linear response of the time-dependent external field in the small amplitude limit. The present method is able to be applied to the effective interactions with density-dependent couplings, in which case the traditional method of equation of motion may fail [90].

First of all, we make a convention for the notations of the single-particle states. Namely the letters a, b, \dots and the capital ones A, B, \dots are used to denote the occupied (hole) and unoccupied (particle) states, respectively. It should be noted that the particle states include both in the Fermi sea and Dirac sea. The letters i, j, \dots are used for general cases.

The details of deriving the RPA equation are given in Appendix B. Here, we just present the RPA eigen equations in the matrix form as

$$\sum_{Bb} \begin{pmatrix} \mathcal{A}_{Aa,Bb} & \mathcal{B}_{Aa,Bb} \\ -\mathcal{B}_{Aa,Bb} & -\mathcal{A}_{Aa,Bb} \end{pmatrix} \begin{pmatrix} X_{Bb} \\ Y_{Bb} \end{pmatrix} = \omega \begin{pmatrix} X_{Aa} \\ Y_{Aa} \end{pmatrix}, \quad (5)$$

where the RPA matrix elements \mathcal{A} and \mathcal{B} read as

$$\mathcal{A}_{12,34} = (\varepsilon_1 - \varepsilon_2)\delta_{12,34} + \sum_\phi \sum_{i=1}^{14} H_i^\phi(1234), \quad (6a)$$

$$\mathcal{B}_{12,34} = - \sum_\phi \sum_{i=1}^{14} H_i^\phi(1243). \quad (6b)$$

In the RPA matrix elements \mathcal{A} and \mathcal{B} , ε_i is the single-particle energy, and H_i^ϕ corresponds to the ph residual interaction of the coupling channel ϕ , which contain totally 14 terms

($i = 1, 2, \dots, 14$). More details about H^ϕ are referred to Appendix C.

2. RPA equations in angular-momentum coupled form

For the nuclei with spherical symmetry, the single-particle states are denoted by $|njl m\rangle$, where n , l , and j represent the principle quantum number, orbital, and total angular momenta, respectively, and m is the projection. Due to the spherical symmetry, the states with the same njl but different m are degenerated, sharing the same radial wave functionals. Thus, the angular integrations in the RPA matrix elements \mathcal{A} and \mathcal{B} in Eq. (5) can be obtained analytically via the angular momentum algebra. Here, we derive the RPA equations in the angular-momentum coupled form [19,91], which is convenient as will be shown later.

Supposing that the external field $W(\mathbf{r})$ has specific angular momentum and parity, i.e., $W(\mathbf{r}) = W_{J^\pi M}(\mathbf{r})$, the angular-momentum coupled X and Y amplitudes can be accordingly defined as follows:

$$X_{Bb}^J = \sum_{m_B m_b} (-1)^{j_b - m_b} C_{j_B m_B, j_b - m_b}^{JM} X_{B m_B, b m_b}, \quad (7a)$$

$$Y_{Bb}^J = \sum_{m_B m_b} (-1)^{j_b - m_b + M} C_{j_B m_B, j_b - m_b}^{J-M} Y_{B m_B, b m_b}, \quad (7b)$$

where $\hat{J} = \sqrt{2J+1}$ and the minus sign in $-m_b$ comes from the fact that the single-particle state b corresponds to the hole state. Meanwhile, the RPA matrix elements in the angular-momentum coupled form are defined as

$$\begin{aligned} \mathcal{A}_{Aa, Bb}^J &= \sum_{mM} (-1)^{j_a - m_a + j_b - m_b} \hat{J}^{-2} C_{j_A m_A, j_a - m_a}^{JM} \\ &\quad \times C_{j_B m_B, j_b - m_b}^{JM} \mathcal{A}_{Aa, Bb}, \end{aligned} \quad (8a)$$

$$\begin{aligned} \mathcal{B}_{Aa, Bb}^J &= \sum_{mM} (-1)^{j_a - m_a + j_b - m_b + M} \hat{J}^{-2} C_{j_A m_A, j_a - m_a}^{JM} \\ &\quad \times C_{j_B m_B, j_b - m_b}^{J-M} \mathcal{B}_{Aa, Bb}, \end{aligned} \quad (8b)$$

where the sum over m represents all the sum over the projections m_A , m_a , m_B , and m_b .

With Eqs. (7) and (8), the RPA eigenequation [Eq. (5)] can be transformed into the angular-momentum coupled form, which reads

$$\sum_{Bb} \begin{pmatrix} \mathcal{A}_{Aa, Bb}^J & \mathcal{B}_{Aa, Bb}^J \\ -\mathcal{B}_{Aa, Bb}^J & -\mathcal{A}_{Aa, Bb}^J \end{pmatrix} \begin{pmatrix} X_{Bb}^J \\ Y_{Bb}^J \end{pmatrix} = \omega \begin{pmatrix} X_{Aa}^J \\ Y_{Aa}^J \end{pmatrix}. \quad (9)$$

3. RPA equations in charge-exchange channels

In this work, we focus on the charge-exchange excitations. Thus, two kinds of ph configurations should be considered, i.e., the proton-particle-neutron-hole configurations and neutron-particle-proton-hole ones. The particle and hole proton (neutron) states are denoted as p and \bar{p} (n and \bar{n}), respectively. The $p\bar{n}$ and $n\bar{p}$ configurations correspond to the isospin lowering T_- and raising T_+ channels, respectively. With this convention, the RPA equation in the angular-momentum

coupled form in Eq. (9) can be expressed explicitly as

$$\begin{aligned} &\sum_{p'\bar{n}'\bar{p}'} \begin{pmatrix} \mathcal{A}_{p\bar{n}'\bar{p}'}^J & \mathcal{A}_{n\bar{p}'\bar{p}'}^J & \mathcal{B}_{p\bar{n}'\bar{p}'}^J & \mathcal{B}_{n\bar{p}'\bar{p}'}^J \\ \mathcal{A}_{n\bar{p}'\bar{p}'}^J & \mathcal{A}_{p\bar{n}'\bar{p}'}^J & \mathcal{B}_{n\bar{p}'\bar{p}'}^J & \mathcal{B}_{p\bar{n}'\bar{p}'}^J \\ -\mathcal{B}_{p\bar{n}'\bar{p}'}^J & -\mathcal{B}_{n\bar{p}'\bar{p}'}^J & -\mathcal{A}_{p\bar{n}'\bar{p}'}^J & -\mathcal{A}_{n\bar{p}'\bar{p}'}^J \\ -\mathcal{B}_{n\bar{p}'\bar{p}'}^J & -\mathcal{B}_{p\bar{n}'\bar{p}'}^J & -\mathcal{A}_{n\bar{p}'\bar{p}'}^J & -\mathcal{A}_{p\bar{n}'\bar{p}'}^J \end{pmatrix} \begin{pmatrix} X_{p'\bar{n}'}^J \\ X_{n'\bar{p}'}^J \\ Y_{p'\bar{n}'}^J \\ Y_{n'\bar{p}'}^J \end{pmatrix} \\ &= \omega \begin{pmatrix} X_{p\bar{n}}^J \\ X_{n\bar{p}}^J \\ Y_{p\bar{n}}^J \\ Y_{n\bar{p}}^J \end{pmatrix}. \end{aligned} \quad (10)$$

Due to the charge conservation, the matrix elements $\mathcal{A}_{p\bar{n}'\bar{p}'}^J$, $\mathcal{A}_{n\bar{p}'\bar{p}'}^J$, $\mathcal{B}_{p\bar{n}'\bar{p}'}^J$, $\mathcal{B}_{n\bar{p}'\bar{p}'}^J$, and $\mathcal{B}_{p\bar{n}'\bar{p}'}^J$ shall vanish. Thus, the RPA equation can be reduced as

$$\begin{aligned} &\sum_{p'\bar{n}'\bar{p}'} \begin{pmatrix} \mathcal{A}_{p\bar{n}'\bar{p}'}^J & 0 & 0 & \mathcal{B}_{p\bar{n}'\bar{p}'}^J \\ 0 & \mathcal{A}_{n\bar{p}'\bar{p}'}^J & \mathcal{B}_{n\bar{p}'\bar{p}'}^J & 0 \\ 0 & -\mathcal{B}_{p\bar{n}'\bar{p}'}^J & -\mathcal{A}_{p\bar{n}'\bar{p}'}^J & 0 \\ -\mathcal{B}_{n\bar{p}'\bar{p}'}^J & 0 & 0 & -\mathcal{A}_{n\bar{p}'\bar{p}'}^J \end{pmatrix} \begin{pmatrix} X_{p'\bar{n}'}^J \\ X_{n'\bar{p}'}^J \\ Y_{p'\bar{n}'}^J \\ Y_{n'\bar{p}'}^J \end{pmatrix} \\ &= \omega \begin{pmatrix} X_{p\bar{n}}^J \\ X_{n\bar{p}}^J \\ Y_{p\bar{n}}^J \\ Y_{n\bar{p}}^J \end{pmatrix}. \end{aligned} \quad (11)$$

Obviously, the T_- and T_+ channels can be obtained simultaneously by solving the following equations:

$$\begin{pmatrix} \mathcal{A}_{p\bar{n}'\bar{p}'}^J & \mathcal{B}_{p\bar{n}'\bar{p}'}^J \\ -\mathcal{B}_{n\bar{p}'\bar{p}'}^J & -\mathcal{A}_{n\bar{p}'\bar{p}'}^J \end{pmatrix} \begin{pmatrix} U_{p'\bar{n}'}^J \\ V_{n'\bar{p}'}^J \end{pmatrix} = \omega \begin{pmatrix} U_{p\bar{n}}^J \\ V_{n\bar{p}}^J \end{pmatrix}. \quad (12)$$

The solutions for the two channels can be distinguished according to the normalization conditions:

$$\sum_{p\bar{n}} (U_{p\bar{n}}^J)^2 - \sum_{n\bar{p}} (V_{n\bar{p}}^J)^2 = +1, \quad T_- \text{ channel}, \quad (13)$$

$$\sum_{p\bar{n}} (U_{p\bar{n}}^J)^2 - \sum_{n\bar{p}} (V_{n\bar{p}}^J)^2 = -1, \quad T_+ \text{ channel}.$$

Meanwhile, the corresponding excitation energies and the X^J and Y^J amplitudes are determined by the following relationship:

$$\begin{aligned} \Omega &= +\omega, \quad X_{p\bar{n}}^J = U_{p\bar{n}}^J, \quad Y_{n\bar{p}}^J = V_{n\bar{p}}^J, \quad T_- \text{ channel}, \\ \Omega &= -\omega, \quad X_{n\bar{p}}^J = V_{n\bar{p}}^J, \quad Y_{p\bar{n}}^J = U_{p\bar{n}}^J, \quad T_+ \text{ channel}. \end{aligned} \quad (14)$$

The most critical step in solving the RPA equation [Eq. (12)] is to calculate the RPA matrix elements \mathcal{A}^J and \mathcal{B}^J . The details about the calculation can be referred to Appendix C.

4. Transition probabilities

Formally, the excited state $|\nu\rangle$, which is the eigenstate of the system Hamiltonian, can be obtained by acting an operator Q_ν^\dagger on the ground state $|\text{GS}\rangle$. In the RPA framework, Q_ν^\dagger can

be expressed with the eigenvector of the RPA equation as

$$Q_v^\dagger = \sum_{pm_p hm_h} X_{ph}^v c_p^\dagger c_h + \sum_{pm_p hm_h} Y_{ph}^v c_h^\dagger c_p. \quad (15)$$

Notice that the ground state here is not the Hartree-Fock ground state $|\text{HF}\rangle \equiv |\Phi\rangle$, but the so-called RPA ground state $|\text{RPA}\rangle$ [90], which satisfies

$$|v\rangle = Q_v^\dagger |\text{RPA}\rangle, \quad Q_v |\text{RPA}\rangle = 0. \quad (16)$$

An operator \hat{f} with specific angular momentum J and M can be expressed with the second-quantized form as

$$\hat{F}_{JM} = \sum_{ij} \langle i | \hat{f}_{JM} | j \rangle c_i^\dagger c_j. \quad (17)$$

For the charge-exchange excitations IAS, GTR, and SDR, the operator \hat{f} reads as

$$\hat{f}_{\text{IAS}}^\pm = \sum_{i=1}^A \tau_\pm(i), \quad (18a)$$

$$\hat{f}_{\text{GTR}}^\pm = \sum_{i=1}^A [1 \otimes \sigma(i)]_{J=1} \tau_\pm(i), \quad (18b)$$

$$\hat{f}_{\text{SDR}}^\pm = \sum_{i=1}^A [r_i Y_1(i) \otimes \sigma(i)]_{J=(0,1,2)} \tau_\pm(i), \quad (18c)$$

where $J = 0$ in the IAS, and $\tau_\pm = \tau_x \pm i\tau_y$.

With the angular-momentum coupled amplitudes X^J and Y^J [Eq. (7)], as well as the Wigner-Eckart theorem [92], one can expand the transition amplitude as

$$\langle v_{JM} | \hat{F}_{JM} | \text{RPA} \rangle = \hat{f}^{-1} \sum_{ph} \{ X_{ph}^{Jv} \langle p | \hat{f}_J | h \rangle + (-1)^{j_p+j_h} Y_{ph}^{Jv} \langle h | \hat{f}_J | p \rangle \}. \quad (19)$$

In deriving Eq. (19), the quasiboson approximation [90] has been adopted, namely, the RPA ground state $|\text{RPA}\rangle$ is approximated as the Hartree-Fock one $|\text{HF}\rangle$,

$$\langle v_{JM} | c_i^\dagger c_j | \text{RPA} \rangle = \sum_{pm_p hm_h} \langle \text{RPA} | [X_{ph}^v c_p^\dagger c_h + Y_{ph}^v c_h^\dagger c_p, c_i^\dagger c_j] | \text{RPA} \rangle$$

$$\begin{aligned} H_{1,t}^{J,\text{PV}}(1234) &= \mathcal{I} \hat{f}^{-2} m_\phi^2 \iint dr_1 dr_2 \mathcal{F}_\phi(1,2) \sum_{L_1 L_2}^{J \pm 1} (-1)^{L_1+L_2} C_{J010}^{L_1 0} C_{J010}^{L_2 0} \\ &\times \left[-R_{L_1 L_2}(m_\phi; r_1, r_2) + \frac{1}{m_\phi^2 r_1^2} \delta(r_1 - r_2) \right] [G_1 G_2 \langle 1 \| \mathcal{T}_{J L_1} \| 2 \rangle]_{r_1} [G_3 G_4 \langle 3 \| \mathcal{T}_{J L_2} \| 4 \rangle]_{r_2} \\ &- \mathcal{I} \frac{1}{3} \hat{f}^{-2} \sum_L \iint dr_1 dr_2 \frac{1}{r_1^2} \delta(r_1 - r_2) \mathcal{F}_\phi(1,2) [G_1 G_2 \langle 1 \| \mathcal{T}_{J L} \| 2 \rangle]_{r_1} [G_3 G_4 \langle 3 \| \mathcal{T}_{J L} \| 4 \rangle]_{r_2} \\ &+ \mathcal{I} \frac{m_\phi^2}{3} \hat{f}^{-2} \sum_L \iint dr_1 dr_2 \mathcal{F}_\phi(1,2) [G_1 G_2 \langle 1 \| \mathcal{T}_{J L} \| 2 \rangle]_{r_1} R_{LL}(m_\phi; r_1, r_2) [G_3 G_4 \langle 3 \| \mathcal{T}_{J L} \| 4 \rangle]_{r_2}, \quad (23) \end{aligned}$$

$$\begin{aligned} &\approx \sum_{pm_p hm_h} \langle \text{HF} | [X_{ph}^v c_h^\dagger c_p + Y_{ph}^v c_p^\dagger c_h, c_i^\dagger c_j] | \text{HF} \rangle \\ &= \sum_{pm_p hm_h} \{ X_{ph}^v \delta_{ip} \delta_{jh} - Y_{ph}^v \delta_{ih} \delta_{jp} \}. \quad (20) \end{aligned}$$

The transition probability between the ground state and the excited state induced by the single-particle operator \hat{F}_{JM} reads

$$B_v = |\langle v_{JM} | \hat{F}_{JM} | \text{RPA} \rangle|^2. \quad (21)$$

To obtain a smooth transition strength as a function of the excitation energy, one usually chooses to calculate the Lorentzian-averaged strength distribution, which reads

$$R(E) = \sum_v B_v \frac{\Gamma/2\pi}{(E - \Omega_v)^2 + \Gamma^2/4}, \quad (22)$$

where Γ is the averaging width.

C. Contribution of tensor force

As mentioned before, the tensor force components can be introduced naturally via the Fock terms, but mixed together with other components. In Ref. [85], the tensor force components in relevant meson-nucleon coupling channels have been identified within the RHF theory. In this work, the same method will be used to extract the contributions from the tensor force components on the RHF level. To avoid confusion, here we make it clear that the two-particle-two-hole effects of tensor force [93–98] are not explicitly taken into account, but implicitly absorbed into the effective interactions to some extent.

In the RHF + RPA framework, the tensor force can also contribute to the RPA ph residual interactions. In Ref. [85], two sets of formulas were given to extract the tensor-force contribution in the two-body interaction matrix elements. These two sets of formulas have the pseudovector and tensor forms, respectively, and they were shown to be identical. Accordingly, we can get two sets of formulas to evaluate the tensor-force contributions to the RPA matrix elements, also with the pseudovector (PV) and tensor (T) forms, respectively. For the charge-exchange excitations, only the regular terms $H_1^J(1234)$ and $H_8^J(1234)$ (see Appendix C) have nonvanishing contributions, while all the rearrangement terms due to the density dependence vanish [71,90,99,100]. Here, we will present specifically the tensor-force contributions to $H_1^J(1234)$, since the ones to $H_8^J(1234)$ can be derived straightforwardly with the relationship shown in Eq. (C6c). The formulas with the PV and T forms, denoted, respectively, as $H_{1,t}^{J,\text{PV}}(1234)$ and $H_{1,t}^{J,\text{T}}(1234)$, can be expressed as,

and

$$\begin{aligned}
H_{1,t}^{J,T}(1234) = & -\mathcal{I}6\hat{f}^{-2}m_\phi^2 \iint dr_1 dr_2 \mathcal{F}_\phi(1,2) \sum_L \sum_{L_1 L_2}^{J \pm 1} (-1)^{L_1+L_2} C_{L_0 10}^{L_1 0} C_{L_0 10}^{L_2 0} \left\{ \begin{matrix} 1 & L_1 & L \\ J & 1 & 1 \end{matrix} \right\} \left\{ \begin{matrix} 1 & L_2 & L \\ J & 1 & 1 \end{matrix} \right\} \\
& \times \left[-R_{L_1 L_2}(m_\phi; r_1, r_2) + \frac{1}{m_\phi^2 r_1^2} \delta(r_1 - r_2) \right] [G_1 G_2 \langle 1 \| \mathcal{T}_{JL_1} \| 2 \rangle]_{r_1} [G_3 G_4 \langle 3 \| \mathcal{T}_{JL_2} \| 4 \rangle]_{r_2} \\
& + \mathcal{I} \frac{2}{3} \hat{f}^{-2} \sum_L \iint dr_1 dr_2 \delta(r_1 - r_2) \mathcal{F}_\phi(1,2) \frac{1}{r_1^2} [G_1 G_2 \langle 1 \| \mathcal{T}_{JL} \| 2 \rangle]_{r_1} [G_3 G_4 \langle 3 \| \mathcal{T}_{JL} \| 4 \rangle]_{r_2} \\
& - \mathcal{I} \frac{2}{3} \hat{f}^{-2} m_\phi^2 \sum_L \iint dr_1 dr_2 \mathcal{F}_\phi(1,2) [G_1 G_2 \langle 1 \| \mathcal{T}_{JL} \| 2 \rangle]_{r_1} R_{LL}(m_\phi, r_1, r_2) [G_3 G_4 \langle 3 \| \mathcal{T}_{JL} \| 4 \rangle]_{r_2}. \quad (24)
\end{aligned}$$

The definition of $R_{L_1 L_2}$ reads

$$\begin{aligned}
R_{L_1 L_2}(m_\phi; r_1, r_2) \equiv & m_\phi \sqrt{\frac{1}{z_1 z_2}} [I_{L_1 + \frac{1}{2}}(z_1) K_{L_2 + \frac{1}{2}}(z_2) \theta(z_2 - z_1) \\
& + K_{L_1 + \frac{1}{2}}(z_1) I_{L_2 + \frac{1}{2}}(z_2) \theta(z_1 - z_2)], \quad (25)
\end{aligned}$$

with $z = m_\phi r$, I and K being the spherical Bessel functions [101], and θ the step function. The reduced matrix element $\langle a \| \mathcal{T}_{JL} \| b \rangle$ is explicitly expressed as

$$\langle a \| \mathcal{T}_{JL} \| b \rangle = (-1)^{l_b} \left(\frac{6}{4\pi} \right)^{1/2} \hat{j}_b \hat{l}_a \hat{l}_b \hat{f} C_{l_a 0 l_b 0}^{L 0} \left\{ \begin{matrix} j_a & j_b & J \\ l_a & l_b & L \\ 1/2 & 1/2 & 1 \end{matrix} \right\}, \quad (26)$$

where j and l are the total and orbital angular momentums. In Eqs. (23) and (24), ϕ represent the coupling channels ω -V, π -PV, ρ -V, ρ -T, and ρ -VT, and the details for \mathcal{F}_ϕ are shown in Table I. The symbol \mathcal{I} in Eqs. (23) and (24) represents the isospin factor, i.e.,

$$\mathcal{I} = \begin{cases} \delta_{q_1 q_2} \delta_{q_3 q_4}, & \text{isoscalar meson;} \\ \langle q_1 | \vec{\tau} | q_2 \rangle \cdot \langle q_4 | \vec{\tau} | q_3 \rangle, & \text{isovector meson,} \end{cases} \quad (27)$$

where $|q_i\rangle$ denotes the isospin spinor of the state $|i\rangle$.

III. RESULTS AND DISCUSSION

A. Isobaric analog state

The IAS belongs to the simplest isospin excitations in nuclei, which is characterized by the quantum numbers $\Delta S = 0$, $\Delta L = 0$, and $\Delta J^\pi = 0^+$. The IAS can be defined by acting the isospin lowering T_- or raising T_+ operators on the

TABLE I. Expressions of \mathcal{F}_ϕ in Eqs. (23) and (24) for the meson-nucleon coupling channels $\phi = \omega$ -V, π -PV, ρ -V, ρ -T, and ρ -VT, in which the M^* is the Dirac mass [60,102].

ϕ	\mathcal{F}_ϕ	ϕ	\mathcal{F}_ϕ
ω -V	$\frac{g_\omega(1)g_\omega(2)}{4M^*(1)M^*(2)}$	π -PV	$-\frac{f_\pi(1)f_\pi(2)}{m_\pi^2}$
ρ -V	$\frac{g_\rho(1)g_\rho(2)}{4M^*(1)M^*(2)}$	ρ -T	$\frac{f_\rho(1)f_\rho(2)}{4M^2}$
		ρ -VT	$\frac{f_\rho(1)g_\rho(2)}{4MM^*(2)} + (1 \leftrightarrow 2)$

parent states, i.e., $T_\pm | \text{parent} \rangle$. When the Coulomb interaction is switched off, the system Hamiltonian commutes with T_- and T_+ (neglecting the tiny isospin-symmetry-breaking components in the nuclear interaction). In this case, the IAS defined by $T_- | \text{parent} \rangle$ and $T_+ | \text{parent} \rangle$ are degenerate with the initial state $| \text{parent} \rangle$. Thus, $E_{\text{IAS}} = 0$ MeV, and the IAS transition strength, which is denoted as B^- for the T_- channel, will exhaust 100% of the nonenergy weighted sum rule $(N - Z)$ [103].

The degeneracy mentioned above is broken in the mean-field approach, since the single-particle Hamiltonian no longer commutes with T_\pm . However, this broken isospin symmetry can be restored by the self-consistent RPA approaches [90,104]. In return, the IAS energy and the transition strength can provide a rigorous test for the self-consistency of the HF + RPA calculations.

To test the self-consistency of the RHF + RPA approach with the presence of the ρ -T coupling, we first calculate the IAS energies and the corresponding transition strengths in doubly magic nuclei ^{48}Ca , ^{90}Zr , and ^{208}Pb by using the effective interaction PKA1, in which the Coulomb interaction is switched off. The results are shown in Table II. It is found that the excitation energies of IAS are all of the order of 10^{-4} MeV. Meanwhile, the strengths exhaust more than 99.9999% of the corresponding sum rule values $(N - Z)$. This indicates that the RHF + RPA approach with ρ -T coupling developed in this work is of excellent self-consistency and also of high numerical accuracy.

By switching off the ph residual interactions from various meson-nucleon couplings one by one, one can evaluate the role played by the relevant channel in deducing zero IAS excitation energy. Figure 1 shows the IAS excitation energy E (MeV) and the transition probability B^- of ^{208}Pb calculated

TABLE II. IAS excitation energies E_{IAS} (MeV) and the corresponding transition probabilities B^- in ^{48}Ca , ^{90}Zr , and ^{208}Pb . The calculations are performed by the RHF+RPA approach with the effective interaction PKA1 [61], where the Coulomb interaction is switched off.

	^{48}Ca	^{90}Zr	^{208}Pb
E_{IAS}	-0.000371	-0.000310	-0.000163
B^-	8.000000	10.000000	43.999990

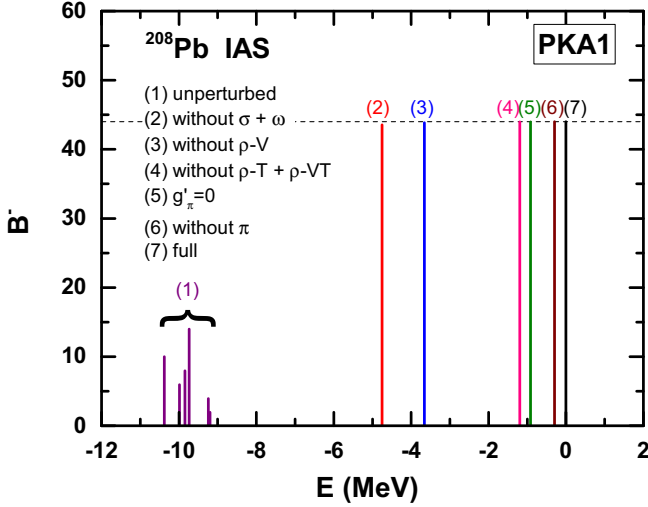


FIG. 1. IAS excitation energies E and transition probabilities B^- in ^{208}Pb calculated by RHF + RPA with PKA1 without the Coulomb interaction. From left to right, the unperturbed result, the ones which exclude the contributions from specific coupling channels in the ph residual interactions, and the full self-consistent calculation are shown. See the text for details.

by PKA1. For comparison, the results of the unperturbed calculation (without residual interaction), the ones which exclude the σ -S + ω -V, ρ -V, ρ -T + ρ -VT, the π contact term ($g'_\pi = 0$) and π -PV couplings, and the fully self-consistent calculation are shown from the left to the right. It can be seen that the isoscalar σ -S and ω -V couplings, as well as the isovector ρ -V one, play the most important role in restoring the isospin symmetry via the ph residual interactions. The π -PV coupling also plays certain role, but not as remarkable as the mentioned ones. Qualitatively, these are in consistence with the PKO1 calculations [100]. In particular, it can be found in Fig. 1 that the ρ -T and ρ -VT couplings play more significant role than the π -PV one.

Moreover, it shall be mentioned that the coefficient of the π contact term, denoted by g'_π , is not a free parameter any more, which is usually adjusted in the RMF + RPA calculations to give proper excitation energy. Within the RHF + RPA, if the g'_π value in the ph residual interaction is changed from $g'_\pi = 1/3$, the self-consistency can be notably violated. When neglecting the π contact term ($g'_\pi = 0$) in the ph residual interaction, the IAS excitation energy calculated with PKA1 turns out to be around -900 keV, similar as the PKO1 result [71], seeing Fig. 1.

B. Gamow-Teller resonance

The Gamow-Teller resonance is characterized by the quantum numbers $\Delta S = 1$, $\Delta L = 0$, and $J^\pi = 1^+$. We show in Table III the excitation energies E (MeV) and the transition probabilities B^- (in percentage of the sum rule value $3(N - Z)$) of the magic nuclei ^{48}Ca , ^{90}Zr , and ^{208}Pb . The results are calculated by the RHF + RPA method with the RHF Lagrangians PKA1 and PKO i ($i = 1, 2, 3$), as compared to the experimental data [105–108] and the calculations by

TABLE III. GTR excitation energies E (MeV) and the transition probabilities B^- [in percentage of the sum rule value $3(N - Z)$] of the magic nuclei ^{48}Ca , ^{90}Zr , and ^{208}Pb , calculated by the RHF+RPA with PKA1 and PKO i ($i = 1, 2, 3$). For comparison, the experimental data [105–108] and the results given by the RMF+RPA with DD-ME1 [109] are also shown.

	^{48}Ca		^{90}Zr		^{208}Pb	
	E	B^-	E	B^-	E	B^-
Exp.	10.5		15.6 \pm 0.3		19.2 \pm 0.2	60 \sim 70
PKA1	11.85	66.4	17.21	65.1	19.76	60.2
PKO1	10.72	69.4	15.80	68.1	18.15	65.6
PKO2	10.83	66.7	15.99	66.3	18.20	60.5
PKO3	10.42	70.7	15.71	68.9	18.14	67.7
DD-ME1	10.28	72.5	15.81	71.0	19.19	70.6

the RMF + RPA with DD-ME1 [109]. All the results shown in Table III correspond to the main peaks. It is found that the GTR excitation energies given by PKA1 are systematically higher than those by PKO i , and all the RHF + RPA calculations present higher energies than the RMF + RPA ones. The model discrepancy might be related to the different symmetry energies given by the selected models as mentioned in Refs. [110,111], which deserves further careful analysis. However, the transition strengths given by the selected models exhaust 60–70 % of the sum rule values $3(N - Z)$, being consistent with the available experimental data [108].

To clarify the roles played by various channels in determining the ph residual interaction, Fig. 2 shows the transition strength R^- (MeV^{-1}) with respect to the excitation energy

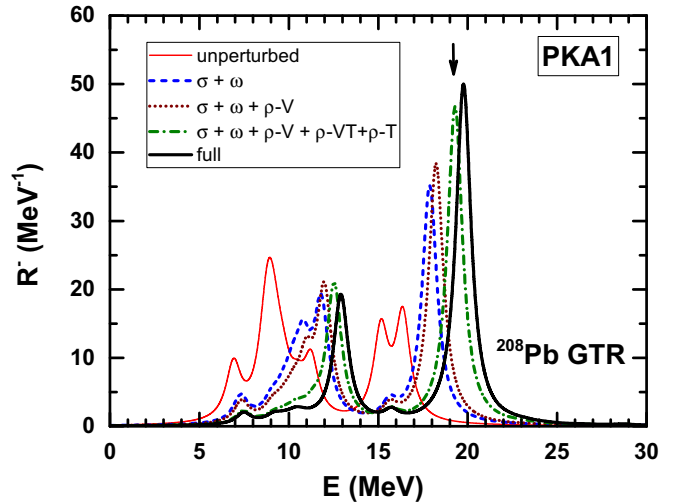


FIG. 2. Transition strength distributions R^- (MeV^{-1}) of GTR in ^{208}Pb with respect to the excitation energy E (MeV) calculated by RHF + RPA with PKA1, including the unperturbed results, the ones of the HF plus the ph residual interactions contributed by relevant channels successively, and the full calculation. A Lorentzian smearing parameter $\Gamma = 1$ MeV is used, and the arrow denotes the experimental peak energy [104]. See the text for details.

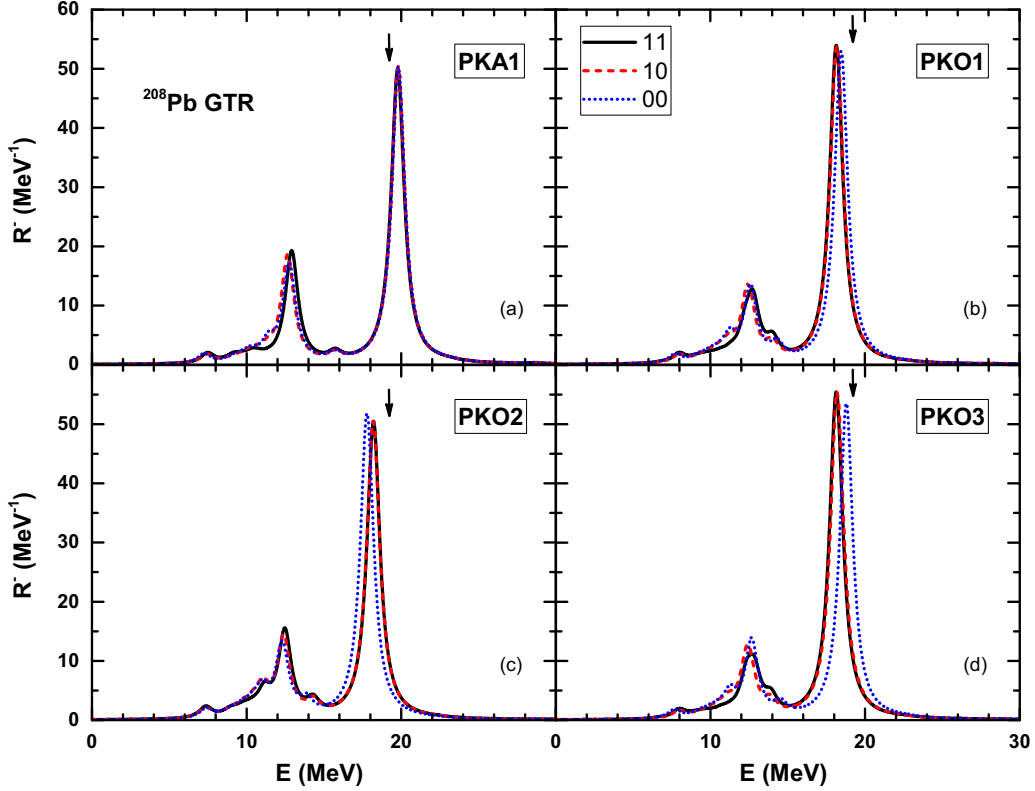


FIG. 3. Transition strength distributions in the T_- channel of GTR in ^{208}Pb calculated by RHF + RPA with PKA1 and PKO i ($i = 1, 2, 3$). A Lorentzian smearing parameter $\Gamma = 1$ MeV is used. The horizontal position of the arrow corresponds to the experimental peak energy [104]. See the text for the meanings of labels 11, 10, and 00.

E (MeV) for ^{208}Pb , including the full self-consistent calculation, the unperturbed one, and the ones of the HF plus the ph residual interactions contributed by the relevant channels successively. The results are calculated by RHF + RPA with PKA1, as referred to the experimental peak energy denoted by the arrow, and a Lorentzian smearing parameter is set as $\Gamma = 1$ MeV. It can be seen that the unperturbed results (thin solid line), in which all the ph residual interactions are dropped, are very far away from the fully self-consistent calculation (thick solid line). If considering the ph residual interaction from the $\sigma + \omega$ channels, then the results are largely improved not only for the excitation energy but also for the transition strength, as referred to the full calculation. Notice that such distinctive improvement is totally due to the Fock diagrams of the σ -S and ω -V couplings [71].

Further considering the contributions to the ph residual interactions from the isovector ρ -V, ρ -T, and π -PV channels successively, the results become gradually closer to the fully self-consistent ones. By comparison one can find that the contribution of the ρ -T coupling channel, together with the accompanying ρ -VT one, is more pronounced than that of the ρ -V and π -PV ones. Similar as the conclusion clarified in Ref. [71], the isoscalar σ -S and ω -V couplings present substantial contributions to the ph residual interactions, fully via the Fock terms. Nevertheless, it is worthwhile to mention that the contributions from the isoscalar channels σ -S and ω -V given by PKA1 are less remarkable, as compared to PKO1 [71], because the balance between the attractive σ -S

and repulsive ω -V couplings is notably changed from PKO1 to PKA1 [81]. Such change is due to the degree of freedom associated with the ρ -T coupling that presents fairly strong attractive potential [81]. Coincidentally, the ρ -T coupling, together with the ρ -VT one, presents significant contributions to the ph residual interactions. Despite of that, the contributions from the ρ -V and π -PV couplings given by both PKA1 and PKO1 [71] are similar.

C. Effects of tensor force on GTR

Within the framework of fully self-consistent RHF + RPA, the tensor force is included naturally in both the RHF mean field and the RPA residual interactions. Thus, the tensor-force effects on the spin-isospin excitations can be manifested in two ways. One is reflected on the single-particle properties (energies and wave functions) via the RHF mean field, further on the RPA calculation. The other influences the RPA calculation directly through the ph residual interactions. In this paper, we mainly focus on the net contribution in specific effective interactions rather than the individual contributions of the relevant meson-nucleon couplings. Taking ^{208}Pb as an example, we explore the effects of tensor force on the GTR, from both the RHF level and RPA level, by performing the following three RHF + RPA calculations:

- (a) tensor force is included in both the RHF and RPA levels, corresponding to the “11” results in Fig. 3;

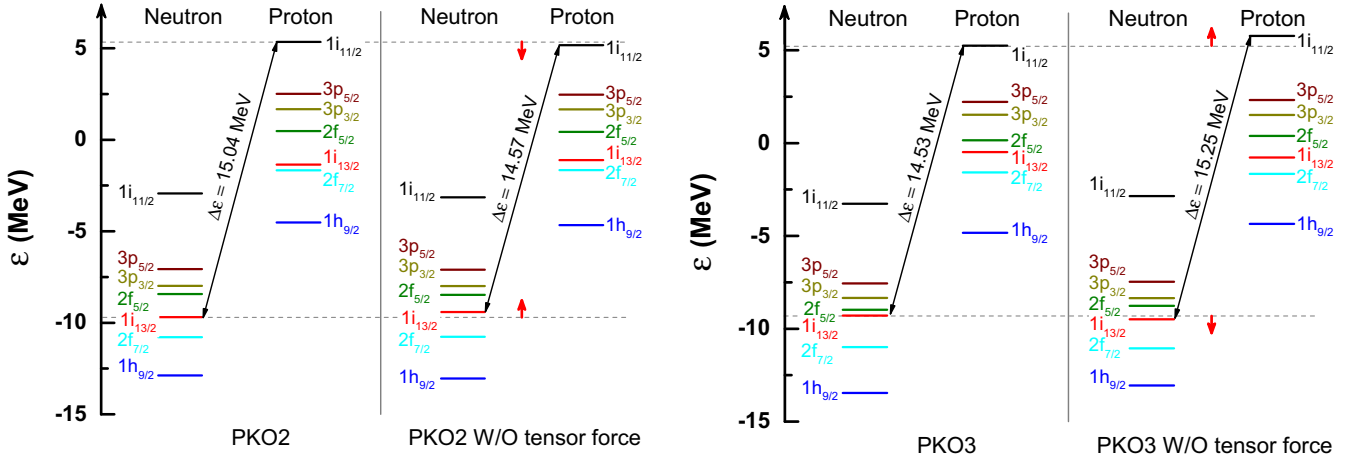


FIG. 4. Neutron and proton single-particle spectrum of ^{208}Pb given by PKO2 (left panel) and PKO3 (right panel), as compared to the ones excluding the tensor force components in the RHF mean fields.

- (b) tensor force is included in RHF but excluded in the RPA level, namely the “10” results in Fig. 3;
- (c) tensor force is excluded in both the RHF and RPA levels, which gives the “00” results in Fig. 3.

The results given by the RHF Lagrangians PKA1 and PKO i are shown in Fig. 3, specifically the excitation energies and transition strengths of the GTR for ^{208}Pb . It is seen that PKA1 shows larger excitation energy for the main peak of ^{208}Pb than the others. Referring to the experimental value (denoted by arrow), it is slightly overestimated by PKA1 while underestimated by PKO i . For ^{48}Ca and ^{90}Zr shown in Table III, it is found that PKO i and DD-ME2 show appropriate agreement with the experimental values on the peak energies, which are overestimated distinctly by PKA1.

Comparing the “10” results to the full ones “11” in Fig. 3, it can be seen that the main peaks given by the selected RHF Lagrangians remain almost unchanged, and the low-energy peaks is only slightly changed. This may indicate that the tensor force components introduced via the Fock terms do not essentially contribute to the ph residual interactions. It is different from the indications from nonrelativistic RPA calculations based on the Skyrme Hartree-Fock theory (SHF + RPA) with the effective interactions SIII and SIII + T, in which the tensor force in the ph residual interactions can bring downwards the main peaks by about 4.1 MeV [46].

Further if the tensor force is excluded on both RHF mean-field and RPA levels, namely, the “00” results in Fig. 3, the main peak given by PKA1 still remains unchanged, while being shifted upwards by about 0.3 MeV and 0.6 MeV for PKO1 and PKO3, respectively, and moving downwards by about 0.4 MeV for PKO2. It is not quite difficult to understand such situation, according to the analysis of the tensor-force effects in Ref. [85]. As already mentioned before, the effective Lagrangian PKA1 contains all the meson-nucleon couplings involved in Eq. (1), i.e., σ -S, ω -V, ρ -V, π -PV, ρ -VT, and ρ -T couplings, whereas the ρ -VT and ρ -T are not contained in PKO i ($i = 1, 2, 3$). Moreover, PKO2 does not contain the π -PV coupling, either. The sign of the tensor force in each

coupling channel is shown in Table I, and more details of their individual effects on the single-particle levels in several isotopic and isotonic chains are referred to Ref. [85]. Thus, for PKO2, only the ω -V and ρ -V couplings contribute to the tensor force components, both of which present opposite effects to the ones carried by the π -PV coupling. For PKO1 and PKO3, the tensor force in π -PV coupling dominates over those from the ω -V and ρ -V couplings to give the net contributions. That is why the tensor-force effects in PKO1 and PKO3 are opposite to those in PKO2. It is also known that the coupling strengths of π -PV is larger in PKO3 than in PKO1, mainly because of its relatively weaker density dependence in the former [60,62]. Consequently, the tensor force in PKO3 affects the properties GTR more profoundly as compared with the case of PKO1. While for PKA1, the tensor-force effects carried by the π -PV coupling are further canceled by the ones carried by the ρ -T and ρ -VT couplings, and hence the net remaining is trivial, leading to unchanged main peak for PKA1. For the nonrelativistic SHF + RPA calculations [46], the main peak is shifted upwards about 0.8 MeV if only neglecting the tensor force in the SHF mean field, qualitatively consistent with the trend of the “00” results given by PKO1 and PKO3.

As discussed above, the tensor force components, introduced naturally via the Fock terms, play different role on the GTR in the RHF + RPA from those in the nonrelativistic SHF + RPA. Specifically for the RHF + RPA, the tensor-force effects on the GTR are manifested mainly via the RHF mean field instead of the ph residual interactions. In contrast to that, for the SHF + RPA [46] the tensor-force effects on the GTR are distinctive via both the SHF mean field and the ph residual interactions, and the latter is dominant. Within the RHF, the tensor-force effects carried by the π -PV couplings are opposite to the ones carried by all the other channels, namely the space components of ω -V, ρ -V, ρ -VT, and ρ -T couplings [85]. For PKA1, the cancellations between the mentioned channels lead to rather weak tensor-force effects, and such cancellations become much less in PKO1 and PKO3, and in PKO2 only opposite tensor-force effects to the ones carried

by the π -PV coupling remain. Thus, one can understand well the discrepancy of the tensor-force effects on the GTR between the RHF Lagrangians.

As a supplement illustration of the tensor-force effects on the GTR, we show in Fig. 4 the neutron and proton single-particle spectra calculated by the RHF Lagrangians PKO2 (left panel) and PKO3 (right panel), in comparison with the self-consistent calculations which exclude the tensor force components introduced via Fock terms. Here, we focus on the occupied neutron orbit $\nu 1i_{13/2}$ and unoccupied proton one $\pi 1i_{11/2}$, which dominate the particle-hole configuration of the main peak of the GTR in ^{208}Pb . As seen from the left panel of Fig. 4, the energy difference given by PKO2 between these two particle-hole partners is $\Delta\varepsilon = 15.04$ MeV, which is reduced about 0.4 MeV when dropping the tensor force components. In contrast to PKO2, the $\Delta\varepsilon$ value given by PKO3 is enlarged about 0.7 MeV when the tensor force components are excluded, seeing the right panel of Fig. 4. Notice that the changes of the energy difference between the particle-hole partners ($\nu 1i_{13/2}$, $\pi 1i_{11/2}$) are consistent with the tensor force components introduced in PKO2 and PKO3 as mentioned before. It is also interesting to see that such modifications are coincident qualitatively with the changes of the position of the main peak for both PKO2 and PKO3, seeing Figs. 3(c) and 3(d).

IV. SUMMARY

In this work, we extend the framework of the random-phase approximation (RPA) based on the relativistic Hartree-Fock (RHF) theory by implementing the degree of freedom associated with the ρ -tensor (ρ -T) coupling, as well as the ρ -vector-tensor (ρ -VT) one. Using the RHF Lagrangian PKA1, good self-consistency of the extended RHF + RPA framework has been illustrated by taking the isobaric analog states (IAS) in ^{48}Ca , ^{90}Zr , and ^{208}Pb as examples. It is found that the ρ -T and ρ -VT couplings play rather important role in keeping the self-consistency of the RHF + RPA calculations, which may indicate substantial contributions from these two channels to the particle-hole (ph) residual interactions.

Further taking ^{48}Ca , ^{90}Zr , and ^{208}Pb as examples, the properties of Gamow-Teller resonances (GTR) are studied by the extended RHF + RPA method, and particular efforts are devoted on the role of the ρ -T coupling and the tensor-force effects. It is shown that appropriate agreements with the available GTR experimental data are achieved by the self-consistent RHF + RPA calculations with PKA1 and PKO*i* ($i = 1, 2, 3$). As compared to the PKO*i* results, the contributions to the ph residual interactions from the isovector channels are notably enhanced by the ρ -T and ρ -VT couplings in PKA1. Moreover, it is found that the tensor-force effects on the GTR, which are introduced naturally by the Fock terms of the relevant channels, are manifested via the RHF mean field instead of the ph residual interaction, which is rather different from the nonrelativistic calculations. In particular, due to the cancellations between the π -PV channel and the others which contain the tensor force components, rather weak tensor-force effects on the GTR are presented by PKA1. In fact, as revealed from the rather different roles played by the tensor force on the GTR between the relativistic and nonrelativistic calculations, it still remains as an important open questions, which may deserve further systematic studies in the future. In addition, it is worthwhile to mention that the individual effects of tensor force from all the relevant couplings can provide valuable guidance for the constraint of the tensor force in a delicate way. Thus, systematic investigation of tensor-force effects on various of spin-isospin excitations is of great interests and significance, which is now in progress.

ACKNOWLEDGMENTS

This work was partly supported by the Natural Science Foundation of China under Grants No. 11905088, No. 11675065, No. 11875152, and No. 11711540016, and the JSPS Grant-in-Aid for Early-Career Scientists under Grant No. 18K13549, and the JSPS Grant-in-Aid for JSPS Fellows under Grant No. 19J20543. The authors also thank Prof. Yifei Niu and Prof. Zhongming Niu for fruitful discussions. Z.W. acknowledges the scholarship of China Scholarship Council, and T.N. and H.L. thank the RIKEN iTHEMS program.

APPENDIX A: TWO-BODY INTERACTIONS IN THE RHF THEORY

In this Appendix, the expressions of the two-body interactions \hat{V}_ϕ in Eq. (4), corresponding to the meson-nucleon couplings σ -S, ω -V, ρ -V, π -PV, ρ -T, and ρ -VT, are shown explicitly:

$$\hat{V}_{\sigma\text{-S}}(1, 2) = g_\sigma(1)g_\sigma(2)I_{\sigma\text{-S}}(1, 2) = -[g_\sigma\gamma_0]_1[g_\sigma\gamma_0]_2D_\sigma(1, 2), \quad (\text{A1a})$$

$$\hat{V}_{\omega\text{-V}}(1, 2) = g_\omega(1)g_\omega(2)I_{\omega\text{-V}}(1, 2) = [g_\omega\gamma_0\gamma^\mu]_1[g_\omega\gamma_0\gamma_\mu]_2D_\omega(1, 2), \quad (\text{A1b})$$

$$\hat{V}_{\rho\text{-V}}(1, 2) = g_\rho(1)g_\rho(2)I_{\rho\text{-V}}(1, 2) = [g_\rho\gamma_0\gamma^\mu\vec{\tau}]_1 \cdot [g_\rho\gamma_0\gamma_\mu\vec{\tau}]_2D_\rho(1, 2), \quad (\text{A1c})$$

$$\hat{V}_{\pi\text{-PV}}(1, 2) = \frac{f_\pi(1)}{m_\pi} \frac{f_\pi(2)}{m_\pi} I_{\pi\text{-PV}}(1, 2) = -\left[\frac{f_\pi}{m_\pi} \gamma_0\gamma_5\vec{\tau}\gamma^k\partial_k \right]_1 \cdot \left[\frac{f_\pi}{m_\pi} \gamma_0\gamma_5\vec{\tau}\gamma^l\partial_l \right]_2 D_\pi(1, 2), \quad (\text{A1d})$$

$$\hat{V}_{\rho\text{-T}}(1, 2) = \frac{f_\rho(1)}{2M} \frac{f_\rho(2)}{2M} I_{\rho\text{-T}}(1, 2) = \left[\frac{f_\rho}{2M} \gamma_0\sigma_{vk}\vec{\tau}\partial^k \right]_1 \cdot \left[\frac{f_\rho}{2M} \gamma_0\sigma^{vl}\vec{\tau}\partial_l \right]_2 D_\rho(1, 2), \quad (\text{A1e})$$

$$\begin{aligned} \hat{V}_{\rho\text{-VT}}(1, 2) &= g_\rho(1) \frac{f_\rho(2)}{2M} I_{\rho\text{-VT}}(1, 2) + \frac{f_\rho(1)}{2M} g_\rho(2) I_{\rho\text{-TV}}(1, 2) \\ &= -[g_\rho\gamma_0\gamma_v\vec{\tau}]_1 \cdot \left[\frac{f_\rho}{2M} \gamma_0\sigma^{vl}\partial_l\vec{\tau} \right]_2 D_\rho(1, 2) - \left[\frac{f_\rho}{2M} \gamma_0\sigma^{vl}\vec{\tau}\partial_l \right]_1 \cdot [g_\rho\gamma_0\gamma_v\vec{\tau}]_2 D_\rho(1, 2). \end{aligned} \quad (\text{A1f})$$

The $D_\phi(1, 2)$ above is the propagators of each coupling, which is of the standard Yukawa form [59]. In addition, to cancel the contact term coming from the π -PV and ρ -T couplings, the zero-range counterterms are included, which read, respectively,

$$\hat{V}_{\pi\text{-PV}}^\delta(1, 2) = \frac{f_\pi(1)}{m_\pi} \frac{f_\pi(2)}{m_\pi} I_{\rho\text{-V}}^\delta(1, 2) = -\frac{1}{3} \left[\frac{f_\pi}{m_\pi} \vec{\tau} \gamma_0 \gamma_5 \gamma^i \right]_1 \cdot \left[\frac{f_\pi}{m_\pi} \vec{\tau} \gamma_0 \gamma_5 \gamma^i \right]_2 \delta(\mathbf{r}_1 - \mathbf{r}_2), \quad (\text{A2a})$$

$$\hat{V}_{\rho\text{-T}}^\delta(1, 2) = \frac{f_\rho(1)}{2M} \frac{f_\rho(2)}{2M} I_{\rho\text{-T}}^\delta(1, 2) = \frac{1}{12M^2} [f_\rho \gamma_0 \sigma_{vi} \vec{\tau}]_1 \cdot [f_\rho \gamma_0 \sigma^{vi} \vec{\tau}]_2 \delta(\mathbf{r}_1 - \mathbf{r}_2). \quad (\text{A2b})$$

APPENDIX B: RPA EQUATION IN GENERAL FORM

Within the density-dependent relativistic Hartree-Fock theory, the single-particle HF equation reads

$$\begin{aligned} \hat{h}_0[\varphi] \varphi_i(1) = & T \varphi_i(1) + \int d\mathbf{r}_2 \left\{ \sum_{\phi, a} \varphi_a^\dagger(2) g_\phi(1) g_\phi(2) I_\phi(1, 2) (1 - P_{ia}) \varphi_a(2) \right\} \varphi_i(1) \\ & + \int d\mathbf{r}_2 \left\{ \sum_{\phi, ab} \varphi_a^\dagger(1) \varphi_b^\dagger(2) \left[\frac{\partial g_\phi(1)}{\partial \rho_b(1)} g_\phi(2) I_\phi(1, 2) (1 - P_{ab}) \right] \varphi_b(2) \varphi_a(1) \right\} \varphi_i(1), \end{aligned} \quad (\text{B1})$$

where ρ_b represents the baryon density, and the operator P_{ij} exchanges the indices i and j . Subjecting the system to a time-dependent external field $\mathcal{W}(t)$, which reads

$$\mathcal{W}(t) = W(\mathbf{r}) e^{-i\omega t} + W^\dagger(\mathbf{r}) e^{i\omega t}, \quad (\text{B2})$$

the single-particle wave functions and the single-particle Hartree-Fock Hamiltonian then change as follows:

$$\varphi_a \rightarrow \psi_a = \varphi_a + \sum_A \beta_{Aa}(t) \varphi_A, \quad (\text{B3a})$$

$$\hat{h}_0[\varphi] \rightarrow \hat{h}_0[\psi] + \mathcal{W}(t). \quad (\text{B3b})$$

Note that the summation over A should run over not only the particle states in the Fermi sea but also those in the Dirac sea. Thus, the time-dependent Hartree-Fock (TDHF) equation becomes

$$i \frac{\partial}{\partial t} \psi_a = (\hat{h}_0[\psi] + \mathcal{W}(t) - \varepsilon_a) \psi_a. \quad (\text{B4})$$

With the small amplitude limit, one can take only the linear response to the external field into account, i.e., only the linear terms of β_{Aa} are kept. Supposing that the expansion coefficients β_{Aa} have the same time-dependent behavior as $\mathcal{W}(t)$, they can be expressed as

$$\beta_{Aa} = X_{Aa} e^{-i\omega t} - Y_{Aa}^* e^{i\omega t}. \quad (\text{B5})$$

Acting a particle state on the TDHF equation [Eq. (B4)] from the left, one can obtain

$$\text{l.h.s.} = \langle \varphi_A | i \frac{\partial}{\partial t} | \psi_a \rangle = i \dot{\beta}_{Aa} = \omega (X_{Aa} e^{-i\omega t} + Y_{Aa}^* e^{i\omega t}) \quad (\text{B6})$$

and

$$\text{r.h.s.} = \langle \varphi_A | \hat{h}_0[\psi] + \mathcal{W}(t) - \varepsilon_a | \varphi_a + \sum_{A'} \beta_{A'a}(t) \varphi_{A'} \rangle. \quad (\text{B7})$$

In the r.h.s. above there appear six individual terms in total. Among them, the first term reads

$$\langle \varphi_A | h_0[\psi] | \varphi_a \rangle = \langle \varphi_A | h_0[\varphi] + \delta h_0 | \varphi_a \rangle. \quad (\text{B8})$$

Because of the orthogonality of the single-particle states, the zero-order term of Eq. (B8), i.e., $\langle \varphi_A | \hat{h}_0[\varphi] | \varphi_a \rangle$, vanishes, and its first-order term reads

$$\langle \varphi_A | \delta h_0 | \varphi_a \rangle = \sum_{\phi, Bb} \{ \beta_{Bb}^* \langle AB | \hat{V}_\phi^{\text{res}}(1, 2) | ab \rangle + \beta_{Bb} \langle Ab | \hat{V}_\phi^{\text{res}}(1, 2) | aB \rangle \}, \quad (\text{B9})$$

where the operator $\hat{V}_\phi^{\text{res}}(1, 2)$ corresponds to the residual particle-hole interaction in the self-consistent RPA approach. As an example, we present the explicit expression of the $\hat{V}_\phi^{\text{res}}(1, 2)$ in the first term of Eq. (B9) as

follows:

$$\begin{aligned}
\hat{V}_\phi^{\text{res}}(1, 2) &= g_\phi(1)g_\phi(2)I_\phi(1, 2)(1 - P_{ab}) + \int d\mathbf{r}_3 \sum_d \varphi_d^\dagger(3) \frac{\partial g_\phi(1)}{\partial \rho_b(1)} g_\phi(3)I_\phi(1, 3)(1 - P_{ad})\varphi_d(3)\delta(\mathbf{r}_1 - \mathbf{r}_2) \\
&+ \sum_d \varphi_d^\dagger(2)g_\phi(1) \frac{\partial g_\phi(2)}{\partial \rho_b(2)} I_\phi(1, 2)(1 - P_{ad})\varphi_d(2) \\
&+ \int d\mathbf{r}_3 \sum_d \varphi_d^\dagger(3) \left[\frac{\partial g_\phi(1)}{\partial \rho_b(1)} g_\phi(3)I_\phi(1, 3)(1 - P_{bd}) \right] \varphi_d(3)\delta(\mathbf{r}_1 - \mathbf{r}_2) \\
&+ \sum_d \varphi_d^\dagger(1) \left[\frac{\partial g_\phi(1)}{\partial \rho_b(1)} g_\phi(2)I_\phi(1, 2)(1 - P_{bd}) \right] \varphi_d(1) \\
&+ \int d\mathbf{r}_3 \sum_{cd} \varphi_c^\dagger(1)\varphi_d^\dagger(3) \frac{\partial^2 g_\phi(1)}{\partial \rho_b^2(1)} g_\phi(3)I_\phi(1, 3)(1 - P_{cd})\varphi_d(3)\varphi_c(1)\delta(\mathbf{r}_1 - \mathbf{r}_2) \\
&+ \sum_{cd} \varphi_c^\dagger(1)\varphi_d^\dagger(2) \frac{\partial g_\phi(1)}{\partial \rho_b(1)} \frac{\partial g_\phi(2)}{\partial \rho_b(2)} I_\phi(1, 2)(1 - P_{cd})\varphi_d(2)\varphi_c(1), \tag{B10}
\end{aligned}$$

of which the first term is the regular term and the others are the rearrangement terms, which arise from the density dependence of the coupling strength. For the second term of Eq. (B9), the operator P_{bd} should be replaced by P_{Bd} . Here, I_ϕ is defined in Eqs. (A1) and (A2). In addition, we emphasize that the derivative of the coupling strength with respect to the density should be evaluated at the ground-state density.

Among the other five terms appearing in the r.h.s., the nonvanishing terms are given as follows:

$$\langle \varphi_A | \mathcal{W} | \varphi_a \rangle = \langle \varphi_A | W(\mathbf{r})e^{-i\omega t} + W^\dagger(\mathbf{r})e^{i\omega t} | \varphi_a \rangle, \tag{B11a}$$

$$\langle \varphi_A | \hat{h}_0 | \psi \rangle \left| \sum_{A'} \beta_{A'a}(t) \varphi_{A'} \right\rangle = \varepsilon_a \beta_{Aa}, \tag{B11b}$$

$$\langle \varphi_A | (-\varepsilon_a) \left| \sum_{A'} \beta_{A'a}(t) \varphi_{A'} \right\rangle = -\varepsilon_a \beta_{Aa}. \tag{B11c}$$

Merging the nonvanishing coefficients of $e^{i\omega t}$ and $e^{-i\omega t}$, respectively, and using the equality of l.h.s. and r.h.s., one can get the following equations:

$$-\langle A | W | a \rangle = [(\varepsilon_A - \varepsilon_a) - \omega] X_{Aa} + \sum_{\phi, Bb} [\langle AB | \hat{V}_\phi^{\text{res}}(1, 2) | aB \rangle X_{Bb} - \langle AB | \hat{V}_\phi^{\text{res}}(1, 2) | ab \rangle Y_{Bb}], \tag{B12a}$$

$$-\langle A | W^\dagger | a \rangle^* = [-(\varepsilon_A - \varepsilon_a) - \omega] Y_{Aa} + \sum_{\phi, Bb} [\langle AB | \hat{V}_\phi^{\text{res}}(1, 2) | ab \rangle X_{Bb} - \langle AB | \hat{V}_\phi^{\text{res}}(1, 2) | aB \rangle Y_{Bb}]. \tag{B12b}$$

The equations above are the RPA equations of X and Y .

With the following compact notation of the ph interaction elements,

$$\mathcal{A}_{12,34} = (\varepsilon_1 - \varepsilon_2)\delta_{12,34} + \sum_\phi \langle 14 | \hat{V}_\phi^{\text{res}} | 23 \rangle, \tag{B13a}$$

$$\mathcal{B}_{12,34} = -\sum_\phi \langle 13 | \hat{V}_\phi^{\text{res}} | 24 \rangle, \tag{B13b}$$

where $\delta_{12,34}$ requires $|1\rangle = |3\rangle$, $|2\rangle = |4\rangle$. The RPA equation above can be rewritten in the matrix form

$$\begin{pmatrix} \mathcal{A}_{Aa, Bb} & \mathcal{B}_{Aa, Bb} \\ -\mathcal{B}_{Aa, Bb} & -\mathcal{A}_{Aa, Bb} \end{pmatrix} \begin{pmatrix} X_{Bb} \\ Y_{Bb} \end{pmatrix} - \omega \begin{pmatrix} X_{Aa} \\ Y_{Aa} \end{pmatrix} = - \begin{pmatrix} \langle A | W | a \rangle \\ \langle A | W^\dagger | a \rangle^* \end{pmatrix}. \tag{B14}$$

The repeated indices B and b indicate the summation over them. Due to the small amplitude limit, the terms on the r.h.s., which is related to the external field, will be dropped. Thus, one gets the RPA eigenequation

$$\begin{pmatrix} \mathcal{A}_{Aa, Bb} & \mathcal{B}_{Aa, Bb} \\ -\mathcal{B}_{Aa, Bb} & -\mathcal{A}_{Aa, Bb} \end{pmatrix} \begin{pmatrix} X_{Bb} \\ Y_{Bb} \end{pmatrix} = \omega \begin{pmatrix} X_{Aa} \\ Y_{Aa} \end{pmatrix}. \tag{B15}$$

APPENDIX C: RPA MATRIX ELEMENTS

From Eq. (B10) one can see that each matrix element $\langle 14|\hat{V}_\phi^{\text{res}}|23\rangle$ contains totally 14 terms, among which the direct terms read as

$$H_1(1234) = \sum_\phi \iint d\mathbf{r}_1 d\mathbf{r}_2 \varphi_1^\dagger(1)\varphi_4^\dagger(2)g_\phi(1)g_\phi(2)I_\phi(1, 2)\varphi_3(2)\varphi_2(1), \quad (\text{C1a})$$

$$H_2(1234) = \sum_{\phi,d} \iint d\mathbf{r}_1 d\mathbf{r}_2 \varphi_1^\dagger(1)\varphi_d^\dagger(2)g'_\phi(1)\varphi_4^\dagger(1)\varphi_3(1)g_\phi(2)I(1, 2)\varphi_d(2)\varphi_2(1), \quad (\text{C1b})$$

$$H_3(1234) = \sum_{\phi,d} \iint d\mathbf{r}_1 d\mathbf{r}_2 \varphi_1^\dagger(1)\varphi_d^\dagger(2)g_\phi(1)g'_\phi(2)\varphi_4^\dagger(2)\varphi_3(2)I(1, 2)\varphi_d(2)\varphi_2(1), \quad (\text{C1c})$$

$$H_4(1234) = \sum_{\phi,d} \iint d\mathbf{r}_1 d\mathbf{r}_2 \varphi_1^\dagger(1)\varphi_4^\dagger(1)\varphi_d^\dagger(2)g'_\phi(1)g_\phi(2)I(1, 2)\varphi_d(2)\varphi_3(1)\varphi_2(1), \quad (\text{C1d})$$

$$H_5(1234) = \sum_{\phi,d} \iint d\mathbf{r}_1 d\mathbf{r}_2 \varphi_1^\dagger(1)\varphi_d^\dagger(1)\varphi_4^\dagger(2)g'_\phi(1)g_\phi(2)I(1, 2)\varphi_3(2)\varphi_d(1)\varphi_2(1), \quad (\text{C1e})$$

$$H_6(1234) = \sum_{\phi,cd} \iint d\mathbf{r}_1 d\mathbf{r}_2 \varphi_1^\dagger(1)\varphi_c^\dagger(1)\varphi_d^\dagger(2)g''_\phi(1)\varphi_4^\dagger(1)\varphi_3(1)g_\phi(2)I(1, 2)\varphi_d(2)\varphi_c(1)\varphi_2(1), \quad (\text{C1f})$$

$$H_7(1234) = \sum_{\phi,cd} \iint d\mathbf{r}_1 d\mathbf{r}_2 \varphi_1^\dagger(1)\varphi_c^\dagger(1)\varphi_d^\dagger(2)g'_\phi(1)g'_\phi(2)\varphi_4^\dagger(2)\varphi_3(2)I(1, 2)\varphi_d(2)\varphi_c(1)\varphi_2(1), \quad (\text{C1g})$$

and the exchange terms read as

$$H_8(1234) = - \sum_\phi \iint d\mathbf{r}_1 d\mathbf{r}_2 \varphi_1^\dagger(1)\varphi_4^\dagger(2)g_\phi(1)g_\phi(2)I_\phi(1, 2)\varphi_2(2)\varphi_3(1), \quad (\text{C2a})$$

$$H_9(1234) = - \sum_{\phi,d} \iint d\mathbf{r}_1 d\mathbf{r}_2 \varphi_1^\dagger(1)\varphi_d^\dagger(2)g'_\phi(1)\varphi_4^\dagger(1)\varphi_3(1)g_\phi(2)I(1, 2)\varphi_2(2)\varphi_d(1), \quad (\text{C2b})$$

$$H_{10}(1234) = - \sum_{\phi,d} \iint d\mathbf{r}_1 d\mathbf{r}_2 \varphi_1^\dagger(1)\varphi_d^\dagger(2)g_\phi(1)g'_\phi(2)\varphi_4^\dagger(2)\varphi_3(2)I(1, 2)\varphi_2(2)\varphi_d(1), \quad (\text{C2c})$$

$$H_{11}(1234) = - \sum_{\phi,d} \iint d\mathbf{r}_1 d\mathbf{r}_2 \varphi_1^\dagger(1)\varphi_4^\dagger(1)\varphi_d^\dagger(2)g'_\phi(1)g_\phi(2)I(1, 2)\varphi_3(2)\varphi_d(1)\varphi_2(1), \quad (\text{C2d})$$

$$H_{12}(1234) = - \sum_{\phi,d} \iint d\mathbf{r}_1 d\mathbf{r}_2 \varphi_1^\dagger(1)\varphi_d^\dagger(1)\varphi_4^\dagger(2)g'_\phi(1)g_\phi(2)I(1, 2)\varphi_d(2)\varphi_3(1)\varphi_2(1), \quad (\text{C2e})$$

$$H_{13}(1234) = - \sum_{\phi,cd} \iint d\mathbf{r}_1 d\mathbf{r}_2 \varphi_1^\dagger(1)\varphi_c^\dagger(1)\varphi_d^\dagger(2)g''_\phi(1)\varphi_4^\dagger(1)\varphi_3(1)g_\phi(2)I(1, 2)\varphi_c(2)\varphi_d(1)\varphi_2(1), \quad (\text{C2f})$$

$$H_{14}(1234) = - \sum_{\phi,cd} \iint d\mathbf{r}_1 d\mathbf{r}_2 \varphi_1^\dagger(1)\varphi_c^\dagger(1)\varphi_d^\dagger(2)g'_\phi(1)g'_\phi(2)\varphi_4^\dagger(2)\varphi_3(2)I(1, 2)\varphi_c(2)\varphi_d(1)\varphi_2(1). \quad (\text{C2g})$$

Notice that $H_1(1234)$ and $H_8(1234)$ belong to the regular terms, whereas the others are the accompanying rearrangement terms. It is notable that, since the effective interactions used in this work only depend on the isoscalar density, the rearrangement terms all vanish in the charge-exchange channels.

In terms of the matrix elements of the direct and exchange terms shown above, the matrix elements $\mathcal{A}_{12,34}^J$ in the angular momentum coupled form defined in Eq. (8a) can be expressed as

$$\mathcal{A}_{12,34}^J = (\varepsilon_1 - \varepsilon_2)\delta_{12,34} + \sum_{i=1}^{14} H_i^J(1234), \quad (\text{C3})$$

where

$$H_i^J(1234) = \sum_{mM} (-1)^{j_2-m_1+j_4-m_3} \frac{1}{\sqrt{2}} C_{j_1 m_1 j_2 -m_2}^{JM} C_{j_3 m_3 j_4 -m_4}^{JM} H_i(1234). \quad (\text{C4})$$

Meanwhile, the matrix elements $\mathcal{B}_{12,34}^J$ in the angular momentum coupled form read

$$\mathcal{B}_{12,34}^J = (-1)^{j_3+j_4} \sum_{i=1}^{14} H_i(1243). \quad (\text{C5})$$

Moreover, $H_i^J(1234)$ satisfies the following relationship:

$$H_4^J(1234) = H_2^J(3412), \quad (\text{C6a})$$

$$H_5^J(1234) = H_3^J(3412), \quad (\text{C6b})$$

$$H_8^J(1234) = (-1)^{j_2+j_3+J+1} \sum_{J'} (-1)^{J'} \hat{J}^2 \begin{Bmatrix} j_2 & j_1 & J \\ j_3 & j_4 & J' \end{Bmatrix} H_1^{J'}(1324), \quad (\text{C6c})$$

$$H_{10}^J(1234) = (-1)^{j_1+j_2+1} H_9^J(2134), \quad (\text{C6d})$$

$$H_{11}^J(1234) = (-1)^{j_3+j_4+1} H_9^J(4312), \quad (\text{C6e})$$

$$H_{12}^J(1234) = H_9^J(3412). \quad (\text{C6f})$$

Thus, all the RPA matrix elements to be calculated explicitly are

$$H_1^J, H_2^J, H_3^J, H_6^J, H_7^J, H_9^J, H_{13}^J, H_{14}^J. \quad (\text{C7})$$

The RHF interactions used in this paper include PKO*i* ($i = 1, 2, 3$) and PKA1, in which the meson-nucleon couplings σ -S, ω -V, ρ -V, π -PV, ρ -T, and ρ -VT are taken into account. Note that the ρ -VT coupling arises simultaneously when ρ -T coupling is included in the Lagrangian. Since this work is focused on the charge-exchange excitations, we prefer to present merely the expressions of the regular term $H_1^J(1234)$ explicitly. The $H_8^J(1234)$ can be derived easily with the relationship shown in Eq. (C6c).

The matrix elements $H_1^J(1234)$ for each meson-nucleon channel, denoted as $H_1^{J\phi}(1234)$, can be eventually expressed as

$$H_1^{J\sigma\text{-S}}(1234) = -\mathcal{I} \hat{J}^{-2} \langle 1 \| Y_L \| 2 \rangle \langle 3 \| Y_L \| 4 \rangle \iint dr_1 dr_2 R_{JJ}(m_\sigma; r_1, r_2) [g_\sigma (G_1 G_2 - F_1 F_2)]_{r_1} [g_\sigma (G_3 G_4 - F_3 F_4)]_{r_2}, \quad (\text{C8a})$$

$$\bar{H}_1^{J\omega\text{-V}}(1234) = -\mathcal{I} \hat{J}^{-2} \langle 1 \| Y_L \| 2 \rangle \langle 3 \| Y_L \| 4 \rangle \iint dr_1 dr_2 R_{JJ}(m_\omega; r_1, r_2) [g_\omega (G_1 G_2 + F_1 F_2)]_{r_1} [g_\omega (G_3 G_4 + F_3 F_4)]_{r_2}, \quad (\text{C8b})$$

$$\begin{aligned} \bar{H}_1^{J\omega\text{-V}}(1234) &= -\mathcal{I} \hat{J}^{-2} \sum_L \iint dr_1 dr_2 R_{LL}(m_\omega, r_1, r_2) \\ &\times [g_\omega (G_1 F_2 \langle 1 \| \mathcal{T}_{JL} \| 2' \rangle - F_1 G_2 \langle 1' \| \mathcal{T}_{JL} \| 2 \rangle)]_{r_1} [g_\omega (G_3 F_4 \langle 3 \| \mathcal{T}_{JL} \| 4' \rangle - F_3 G_4 \langle 3' \| \mathcal{T}_{JL} \| 4 \rangle)]_{r_2}, \end{aligned} \quad (\text{C8c})$$

$$\begin{aligned} H_1^{J\pi\text{-PV}}(1234) &= -\mathcal{I} \hat{J}^{-2} \iint dr_1 dr_2 \sum_{L_1 L_2}^{J \pm 1} (-1)^{L_1+L_2} C_{J010}^{L_1 0} C_{J010}^{L_2 0} \mathcal{V}_J^{L_1 L_2}(m_\pi; r_1, r_2) [f_\pi (G_1 G_2 \langle 1 \| \mathcal{T}_{JL_1} \| 2 \rangle + F_1 F_2 \langle 1' \| \mathcal{T}_{JL_1} \| 2' \rangle)]_{r_1} \\ &\times [f_\pi (G_3 G_4 \langle 3 \| \mathcal{T}_{JL_2} \| 4 \rangle + F_3 F_4 \langle 3' \| \mathcal{T}_{JL_2} \| 4' \rangle)]_{r_2}, \end{aligned} \quad (\text{C8d})$$

$$H_1^{J\pi\text{-PV},\delta}(1234) = \mathcal{I} \frac{1}{3m_\pi^2} \hat{J}^{-2} \sum_L \int dr \frac{f_\pi^2}{r^2} [G_1 G_2 \langle 1 \| \mathcal{T}_{JL} \| 2 \rangle + F_1 F_2 \langle 1' \| \mathcal{T}_{JL} \| 2' \rangle] [G_3 G_4 \langle 3 \| \mathcal{T}_{JL} \| 4 \rangle + F_3 F_4 \langle 3' \| \mathcal{T}_{JL} \| 4' \rangle], \quad (\text{C8e})$$

$$\begin{aligned} \bar{H}_1^{J\rho\text{-T}}(1234) &= \mathcal{I} \hat{J}^{-2} \frac{m_\rho^2}{4M^2} \iint dr_1 dr_2 \sum_{L_1 L_2}^{J \pm 1} (-1)^{L_1+L_2} C_{J010}^{L_1 0} C_{J010}^{L_2 0} \mathcal{V}_J^{L_1 L_2}(m_\rho; r_1, r_2) [f_\rho (F_1 G_2 \langle 1' \| \mathcal{T}_{JL_1} \| 2 \rangle + G_1 F_2 \langle 1 \| \mathcal{T}_{JL_1} \| 2' \rangle)]_{r_1} \\ &\times [f_\rho (G_3 F_4 \langle 3 \| \mathcal{T}_{JL_2} \| 4' \rangle + F_3 G_4 \langle 3' \| \mathcal{T}_{JL_2} \| 4 \rangle)]_{r_2}, \end{aligned} \quad (\text{C8f})$$

$$\bar{H}_1^{J\rho\text{-T},\delta}(1234) = -\mathcal{I} \frac{1}{12M^2} \hat{J}^{-2} \sum_L \int dr \frac{f_\rho^2}{r^2} [G_1 F_2 \langle 1 \| \mathcal{T}_{JL} \| 2' \rangle + F_1 G_2 \langle 1' \| \mathcal{T}_{JL} \| 2 \rangle] [G_3 F_4 \langle 3 \| \mathcal{T}_{JL} \| 4' \rangle + F_3 G_4 \langle 3' \| \mathcal{T}_{JL} \| 4 \rangle], \quad (\text{C8g})$$

$$\begin{aligned} \bar{H}_1^{J\rho\text{-T}}(1234) &= -\mathcal{I} \hat{J}^{-2} \frac{m_\rho^2}{4M^2} \iint dr_1 dr_2 \sum_L \hat{L}^2 \sum_{L_1 L_2}^{L \pm 1} (-1)^{L_1+L_2} C_{L010}^{L_1 0} C_{L010}^{L_2 0} \mathcal{V}_L^{L_1 L_2}(m_\rho; r_1, r_2) \begin{Bmatrix} 1 & L_1 & L \\ J & 1 & 1 \end{Bmatrix} \begin{Bmatrix} 1 & L_2 & L \\ J & 1 & 1 \end{Bmatrix} \\ &\times [f_\rho (G_1 G_2 \langle 1 \| \mathcal{T}_{JL_1} \| 2 \rangle - F_1 F_2 \langle 1' \| \mathcal{T}_{JL_1} \| 2' \rangle)]_{r_1} [f_\rho (G_3 G_4 \langle 3 \| \mathcal{T}_{JL_2} \| 4 \rangle - F_3 F_4 \langle 3' \| \mathcal{T}_{JL_2} \| 4' \rangle)]_{r_2}, \end{aligned} \quad (\text{C8h})$$

$$\bar{H}_1^{J\rho\text{-T},\delta}(1234) = \mathcal{I} \frac{1}{6M^2} \hat{J}^{-2} \sum_L \int dr \frac{f_\rho^2}{r^2} [G_1 G_2 \langle 1 \| \mathcal{T}_{JL} \| 2 \rangle - F_1 F_2 \langle 1' \| \mathcal{T}_{JL} \| 2' \rangle] [G_3 G_4 \langle 3 \| \mathcal{T}_{JL} \| 4 \rangle - F_3 F_4 \langle 3' \| \mathcal{T}_{JL} \| 4' \rangle], \quad (\text{C8i})$$

$$\begin{aligned}
 \bar{H}_1^{J\rho\text{-VT}}(1234) &= \mathcal{I}(-1)^{J+1} \hat{f}^{-2} \frac{m_\rho}{2M} \sum_{L_1}^{J\pm 1} (-1)^{L_1} C_{J010}^{L_1 0} \iint dr_1 dr_2 S_{L_1 J}(m_\rho; r_1, r_2) \\
 &\quad \times [g_\rho \langle 1 \| Y_J \| 2 \rangle (G_1 G_2 + F_1 F_2)]_{r_1} [f_\rho (G_3 F_4 \langle 3 \| \mathcal{T}_{JL_1} \| 4' \rangle + F_3 G_4 \langle 3' \| \mathcal{T}_{JL_1} \| 4 \rangle)]_{r_2} \\
 &+ \mathcal{I}(-1)^J \hat{f}^{-2} \frac{m_\rho}{2M} \sum_{L_1}^{J\pm 1} (-1)^{L_1} C_{J010}^{L_1 0} \iint dr_1 dr_2 S_{JL_1}(m_\rho; r_1, r_2) \\
 &\quad \times [f_\rho (F_1 G_2 \langle 1' \| \mathcal{T}_{JL_1} \| 2 \rangle + G_1 F_2 \langle 1 \| \mathcal{T}_{JL_1} \| 2' \rangle)]_{r_1} [g_\rho \langle 3 \| Y_J \| 4 \rangle (G_3 G_4 + F_3 F_4)]_{r_2}, \tag{C8j}
 \end{aligned}$$

$$\begin{aligned}
 \bar{H}_1^{J\rho\text{-VT}}(1234) &= \mathcal{I}(-1)^{J+1} \frac{\sqrt{6} m_\rho}{2M} \hat{f}^{-2} \sum_L \sum_{L_1}^{L\pm 1} \hat{L} \iint dr_1 dr_2 S_{L_1 L}(m_\rho; r_1, r_2) (-1)^{L_1} C_{L010}^{L_1 0} \begin{Bmatrix} 1 & L_1 & L \\ J & 1 & 1 \end{Bmatrix} \\
 &\quad \times [g_\rho (G_1 F_2 \langle 1 \| \mathcal{T}_{JL} \| 2' \rangle - F_1 G_2 \langle 1' \| \mathcal{T}_{JL} \| 2 \rangle)]_{r_1} [f_\rho (G_3 G_4 \langle 3 \| \mathcal{T}_{JL} \| 4 \rangle - F_3 F_4 \langle 3' \| \mathcal{T}_{JL} \| 4' \rangle)]_{r_2} \\
 &+ \mathcal{I}(-1)^J \frac{\sqrt{6} m_\rho}{2M} \hat{f}^{-2} \sum_L \sum_{L_1}^{L\pm 1} \hat{L} \iint dr_1 dr_2 S_{LL_1}(m_\rho; r_1, r_2) (-1)^{L_1} C_{L010}^{L_1 0} \begin{Bmatrix} 1 & L_1 & L \\ J & 1 & 1 \end{Bmatrix} \\
 &\quad \times [f_\rho (G_1 G_2 \langle 1 \| \mathcal{T}_{JL_1} \| 2 \rangle - F_1 F_2 \langle 1' \| \mathcal{T}_{JL_1} \| 2' \rangle)]_{r_1} [g_\rho (G_3 F_4 \langle 3 \| \mathcal{T}_{JL} \| 4' \rangle - F_3 G_4 \langle 3' \| \mathcal{T}_{JL} \| 4 \rangle)]_{r_2}. \tag{C8k}
 \end{aligned}$$

The isospin factor \mathcal{I} in the expressions above has been defined in Eq. (27). The $H_1^{J\rho\text{-V}}(1234)$ is not shown explicitly, since it can be obtained from $H_1^{J\omega\text{-V}}(1234)$ by replacing the corresponding meson mass, coupling constants, and isospin factor. The reduced matrix element of the spherical harmonic operator presented above reads

$$\langle a \| Y_L \| b \rangle = (-1)^{j_b + \frac{1}{2}} \frac{\hat{j}_a \hat{j}_b}{\sqrt{4\pi}} C_{j_a - \frac{1}{2} j_b \frac{1}{2}}^{L0}, \tag{C9}$$

provided that $l_a + l_b + L$ is even, and zero otherwise. The reduced matrix element of the vector spherical harmonic operator is given in Eq. (26). Besides, one should notice that the spherical harmonic spinors $|a\rangle$ and $|a'\rangle$ have the same total angular momentum j_a , but different orbital ones l_a and l_a' which satisfy the relationship $l_a + l_a' = 2j_a$.

-
- [1] F. Osterfeld, *Rev. Mod. Phys.* **64**, 491 (1992).
 [2] M. Ichimura, H. Sakai, and T. Wakasa, *Prog. Part. Nucl. Phys.* **56**, 446 (2006).
 [3] C. J. Batty, E. Friedman, H. J. Gils, and H. Rebel, in *Advances in Nuclear Physics*, edited by E. Negele and J. W. Vogt (Springer, Boston, MA, 1989) p. 1.
 [4] A. Krasznahorkay *et al.*, *Phys. Rev. Lett.* **82**, 3216 (1999).
 [5] D. Vretenar, N. Paar, T. Nikšić, and P. Ring, *Phys. Rev. Lett.* **91**, 262502 (2003).
 [6] K. Yako, H. Sagawa, and H. Sakai, *Phys. Rev. C* **74**, 051303(R) (2006).
 [7] H. Ejiri, *Phys. Rep.* **338**, 265 (2000).
 [8] K. Langanke and G. Martínez-Pinedo, *Rev. Mod. Phys.* **75**, 819 (2003).
 [9] M. Arnould, S. Goriely, and K. Takahashi, *Phys. Rep.* **450**, 97 (2007).
 [10] Y. Fujita, B. Rubio, and W. Gelletly, *Prog. Part. Nucl. Phys.* **66**, 549 (2011).
 [11] J. Engel, M. Bender, J. Dobaczewski, W. Nazarewicz, and R. Surman, *Phys. Rev. C* **60**, 014302 (1999).
 [12] N. Paar, D. Vretenar, T. Marketin, and P. Ring, *Phys. Rev. C* **77**, 024608 (2008).
 [13] N. Paar, Y. F. Niu, D. Vretenar, and J. Meng, *Phys. Rev. Lett.* **103**, 032502 (2009).
 [14] Z. Niu, B. Sun, and J. Meng, *Phys. Rev. C* **80**, 065806 (2009).
 [15] Y. F. Niu, N. Paar, D. Vretenar, and J. Meng, *Phys. Rev. C* **83**, 045807 (2011).
 [16] Y. F. Niu, G. Colò, M. Brenna, P. F. Bortignon, and J. Meng, *Phys. Rev. C* **85**, 034314 (2012).
 [17] Z. M. Niu, Y. F. Niu, H. Z. Liang, W. H. Long, T. Nikšić, D. Vretenar, and J. Meng, *Phys. Lett. B* **723**, 172 (2013).
 [18] Y. F. Niu, Z. M. Niu, G. Colò, and E. Vigezzi, *Phys. Rev. Lett.* **114**, 142501 (2015).
 [19] Y. F. Niu, G. Colò, E. Vigezzi, C. L. Bai, and H. Sagawa, *Phys. Rev. C* **94**, 064328 (2016).
 [20] Y. F. Niu, Z. M. Niu, G. Colò, and E. Vigezzi, *Phys. Lett. B* **780**, 325 (2018).
 [21] Z. M. Niu, H. Z. Liang, B. H. Sun, W. H. Long, and Y. F. Niu, *Phys. Rev. C* **99**, 064307 (2006).
 [22] N. Cabibbo, *Phys. Rev. Lett.* **10**, 531 (1963).
 [23] M. Kobayashi and T. Maskawa, *Prog. Theor. Phys.* **49**, 652 (1973).
 [24] H. Sagawa, N. Van Giai, and T. Suzuki, *Phys. Rev. C* **53**, 2163 (1996).
 [25] J. C. Hardy and I. S. Towner, *Phys. Rev. C* **71**, 055501 (2005).
 [26] H. Liang, N. V. Giai, and J. Meng, *Phys. Rev. C* **79**, 064316 (2009).
 [27] J. C. Hardy and I. S. Towner, *Phys. Rev. C* **91**, 025501 (2015).
 [28] N. Paar, D. Vretenar, E. Khan, and G. Colò, *Rep. Prog. Phys.* **70**, 691 (2007).

- [29] T. Otsuka, T. Suzuki, R. Fujimoto, H. Grawe, and Y. Akaishi, *Phys. Rev. Lett.* **95**, 232502 (2005).
- [30] I. Tanihata, H. Hamagaki, O. Hashimoto, Y. Shida, N. Yoshikawa, K. Sugimoto, O. Yamakawa, T. Kobayashi, and N. Takahashi, *Phys. Rev. Lett.* **55**, 2676 (1985).
- [31] P. D. Cottle and K. W. Kemper, *Phys. Rev. C* **58**, 3761 (1998).
- [32] J. P. Schiffer, S. J. Freeman, J. A. Caggiano, C. Deibel, A. Heinz, C. L. Jiang, R. Lewis, A. Parikh, P. D. Parker, K. E. Rehm, S. Sinha, and J. S. Thomas, *Phys. Rev. Lett.* **92**, 162501 (2004).
- [33] T. Wakasa, H. Sakai, H. Okamura, H. Otsu, S. Fujita, S. Ishida, N. Sakamoto, T. Uesaka, Y. Satou, M. B. Greenfield, and K. Hatanaka, *Phys. Rev. C* **55**, 2909 (1997).
- [34] T. Wakasa, M. Okamoto, M. Dozono, K. Hatanaka, M. Ichimura, S. Kuroita, Y. Maeda, H. Miyasako, T. Noro, T. Saito, Y. Sakemi, T. Yabe, and K. Yako, *Phys. Rev. C* **85**, 064606 (2012).
- [35] S. Terashima *et al.*, *Phys. Rev. Lett.* **121**, 242501 (2018).
- [36] H. Sagawa and G. Colò, *Prog. Part. Nucl. Phys.* **76**, 76 (2014).
- [37] T. Otsuka, A. Gade, O. Sorlin, T. Suzuki, and Y. Utsuno, *Rev. Mod. Phys.* **92**, 015002 (2020).
- [38] C. L. Bai, H. Q. Zhang, H. Sagawa, X. Z. Zhang, G. Colò, and F. R. Xu, *Phys. Rev. C* **83**, 054316 (2011).
- [39] M. Anguiano, G. Co', V. De Donno, and A. M. Lallena, *Phys. Rev. C* **83**, 064306 (2011).
- [40] E. Litvinova, B. Brown, D.-L. Fang, T. Marketin, and R. Zegers, *Phys. Lett. B* **730**, 307 (2014).
- [41] C. L. Bai, H. Q. Zhang, H. Sagawa, X. Z. Zhang, G. Colò, and F. R. Xu, *Phys. Rev. Lett.* **105**, 072501 (2010).
- [42] P. Hohenberg and W. Kohn, *Phys. Rev.* **136**, B864 (1964).
- [43] W. Kohn and L. J. Sham, *Phys. Rev.* **140**, A1133 (1965).
- [44] W. Kohn, *Rev. Mod. Phys.* **71**, 1253 (1999).
- [45] M. Bender, P. H. Heenen, and P. G. Reinhard, *Rev. Mod. Phys.* **75**, 121 (2003).
- [46] C. L. Bai, H. Sagawa, H. Q. Zhang, X. Z. Zhang, G. Colò, and F. R. Xu, *Phys. Lett. B* **675**, 28 (2009).
- [47] C. L. Bai, H. Q. Zhang, X. Z. Zhang, F. R. Xu, H. Sagawa, and G. Colò, *Phys. Rev. C* **79**, 041301(R) (2009).
- [48] C. L. Bai, H. Sagawa, G. Colò, H. Q. Zhang, and X. Z. Zhang, *Phys. Rev. C* **84**, 044329 (2011).
- [49] D. M. Brink and F. Stancu, *Phys. Rev. C* **75**, 064311 (2007).
- [50] G. Colò, H. Sagawa, S. Fracasso, and P. F. Bortignon, *Phys. Lett. B* **646**, 227 (2007).
- [51] T. Lesinski, M. Bender, K. Bennaceur, T. Duguet, and J. Meyer, *Phys. Rev. C* **76**, 014312 (2007).
- [52] S. Shen, G. Colò, and X. Roca-Maza, *Phys. Rev. C* **99**, 034322 (2019).
- [53] J. Meng, H. Toki, S. G. Zhou, S. Q. Zhang, W. H. Long, and L. S. Geng, *Prog. Part. Nucl. Phys.* **57**, 470 (2006).
- [54] T. Nikšić, D. Vretenar, and P. Ring, *Prog. Part. Nucl. Phys.* **66**, 519 (2011).
- [55] H. Z. Liang, J. Meng, and S. G. Zhou, *Phys. Rep.* **570**, 1 (2015).
- [56] J. Meng, ed., *Relativistic Density Functional for Nuclear Structure*, International Review of Nuclear Physics, Vol. 10 (World Scientific, Singapore, 2016).
- [57] X. W. Xia, Y. Lim, P. W. Zhao, H. Z. Liang, X. Y. Qu, Y. Chen, H. Liu, L. F. Zhang, S. Q. Zhang, Y. Kim, and J. Meng, *At Data Nucl Data Tables* **121-122**, 1 (2018).
- [58] S. Shen, H. Liang, W. H. Long, J. Meng, and P. Ring, *Prog. Part. Nucl. Phys.* **109**, 103713 (2019).
- [59] A. Bouyssy, J. F. Mathiot, N. Van Giai, and S. Marcos, *Phys. Rev. C* **36**, 380 (1987).
- [60] W. H. Long, N. Van Giai, and J. Meng, *Phys. Lett. B* **640**, 150 (2006).
- [61] W. H. Long, H. Sagawa, N. V. Giai, and J. Meng, *Phys. Rev. C* **76**, 034314 (2007).
- [62] W. H. Long, H. Sagawa, J. Meng, and N. Van Giai, *Europhys. Lett.* **82**, 12001 (2008).
- [63] L. J. Wang, J. M. Dong, and W. H. Long, *Phys. Rev. C* **87**, 047301 (2013).
- [64] L. J. Jiang, S. Yang, J. M. Dong, and W. H. Long, *Phys. Rev. C* **91**, 025802 (2015).
- [65] L. J. Jiang, S. Yang, B. Y. Sun, W. H. Long, and H. Q. Gu, *Phys. Rev. C* **91**, 034326 (2015).
- [66] P. Bernardos, V. N. Fomenko, N. V. Giai, M. L. Quelle, S. Marcos, R. Niembro, and L. N. Savushkin, *Phys. Rev. C* **48**, 2665 (1993).
- [67] S. Marcos, L. N. Savushkin, V. N. Fomenko, M. López-Quelle, and R. Niembro, *J. Phys. G: Nucl. Part. Phys.* **30**, 703 (2004).
- [68] W. H. Long, P. Ring, N. Van Giai, and J. Meng, *Phys. Rev. C* **81**, 024308 (2010).
- [69] W. H. Long, T. Nakatsukasa, H. Sagawa, J. Meng, H. Nakada, and Y. Zhang, *Phys. Lett. B* **680**, 428 (2009).
- [70] J. J. Li, J. Margueron, W. H. Long, and N. Van Giai, *Phys. Lett. B* **753**, 97 (2016).
- [71] H. Z. Liang, N. Van Giai, and J. Meng, *Phys. Rev. Lett.* **101**, 122502 (2008).
- [72] H. Z. Liang, P. W. Zhao, and J. Meng, *Phys. Rev. C* **85**, 064302 (2012).
- [73] Z. M. Niu, Y. F. Niu, H. Z. Liang, W. H. Long, and J. Meng, *Phys. Rev. C* **95**, 044301 (2017).
- [74] B. Y. Sun, W. H. Long, J. Meng, and U. Lombardo, *Phys. Rev. C* **78**, 065805 (2008).
- [75] W. H. Long, B. Y. Sun, K. Hagino, and H. Sagawa, *Phys. Rev. C* **85**, 025806 (2012).
- [76] Q. Zhao, B. Y. Sun, and W. H. Long, *J. Phys. G: Nucl. Part. Phys.* **42**, 095101 (2015).
- [77] Z. W. Liu, Z. Qian, R. Y. Xing, J. R. Niu, and B. Y. Sun, *Phys. Rev. C* **97**, 025801 (2018).
- [78] Z. W. Liu, Q. Zhao, and B. Y. Sun, [arXiv:1809.03837](https://arxiv.org/abs/1809.03837).
- [79] J. J. Li, W. H. Long, J. Margueron, and N. Van Giai, *Phys. Lett. B* **788**, 192 (2019).
- [80] W. H. Long, H. Sagawa, J. Meng, and N. Van Giai, *Phys. Lett. B* **639**, 242 (2006).
- [81] J. Geng, J. J. Li, W. H. Long, Y. F. Niu, and S. Y. Chang, *Phys. Rev. C* **100**, 051301(R) (2019).
- [82] W. H. Long, P. Ring, J. Meng, N. Van Giai, and C. A. Bertulani, *Phys. Rev. C* **81**, 031302(R) (2010).
- [83] H. Z. Liang, P. W. Zhao, P. Ring, X. Roca-Maza, and J. Meng, *Phys. Rev. C* **86**, 021302(R) (2012).
- [84] R. Machleidt, *Advances in Nuclear Physics*, edited by J. W. Negele and E. Vogt (Springer, Boston, MA, 1989), Vol. 19, pp. 189–376.
- [85] Z. Wang, Q. Zhao, H. Liang, and W. H. Long, *Phys. Rev. C* **98**, 034313 (2018).
- [86] H. Yukawa, *Proc. Phys. Math. Soc. Japan* **17**, 48 (1935).

- [87] J. D. Walecka, *Ann. Phys.* **83**, 491 (1974).
- [88] W. H. Long, Ph.D. thesis, Peking University, China and Université Paris Sud-Paris XI, France (2005).
- [89] P. Ring, Z.-Y. Ma, N. Van Giai, D. Vretenar, A. Wandelt, and L.-G. Cao, *Nucl. Phys. A* **694**, 249 (2001).
- [90] P. Ring and P. Schuck, *The Nuclear Many-body Problem* (Springer, New York, NY, 1980).
- [91] N. Paar, P. Ring, T. Nikšić, and D. Vretenar, *Phys. Rev. C* **67**, 034312 (2003).
- [92] D. A. Varshalovich, A. N. Moskalev, and V. K. Khersonskii, *Quantum Theory of Angular Momentum* (World Scientific, Singapore, 1988).
- [93] H. Kamada *et al.*, *Phys. Rev. C* **64**, 044001 (2001).
- [94] T. Myo, K. Kat, and K. Ikeda, *Prog. Theor. Phys.* **113**, 763 (2005).
- [95] T. Myo, K. Katō, H. Toki, and K. Ikeda, *Phys. Rev. C* **76**, 024305 (2007).
- [96] Y. Ogawa and H. Toki, *Ann. Phys.* **326**, 2039 (2011).
- [97] T. Myo, H. Toki, K. Ikeda, H. Horiuchi, and T. Suhara, *Phys. Rev. C* **95**, 044314 (2017).
- [98] T. Myo, H. Toki, K. Ikeda, H. Horiuchi, T. Suhara, M. Lyu, M. Isaka, and T. Yamada, *Prog. Theor. Exp. Phys.* **2017**, 111D01 (2017).
- [99] T. Nikšić, D. Vretenar, and P. Ring, *Phys. Rev. C* **66**, 064302 (2002).
- [100] H. Z. Liang, Ph.D. thesis, Peking University, China and Université Paris Sud-Paris XI, France (2005).
- [101] M. Abramowitz and I. A. Stegun, *Handbook of Mathematical Functions: With Formulas, Graphs, and Mathematical Tables* (Dover Publications, New York, NY, 1970).
- [102] L.-J. Wang, Y. Sun, and S. K. Ghorui, *Phys. Rev. C* **97**, 044302 (2018).
- [103] C. A. Engelbrecht and R. H. Lemmer, *Phys. Rev. Lett.* **24**, 607 (1970).
- [104] D. Thouless, *Nucl. Phys.* **22**, 78 (1961).
- [105] B. D. Anderson, T. Chittrakarn, A. R. Baldwin, C. Lebo, R. Madey, P. C. Tandy, J. W. Watson, B. A. Brown, and C. C. Foster, *Phys. Rev. C* **31**, 1161 (1985).
- [106] D. E. Bainum, J. Rapaport, C. D. Goodman, D. J. Horen, C. C. Foster, M. B. Greenfield, and C. A. Goulding, *Phys. Rev. Lett.* **44**, 1751 (1980).
- [107] D. Horen, C. Goodman, C. Foster, C. Goulding, M. Greenfield, J. Rapaport, D. Bainum, E. Sugarbaker, T. Masterson, F. Petrovich, and W. Love, *Phys. Lett. B* **95**, 27 (1980).
- [108] H. Akimune, I. Daito, Y. Fujita, M. Fujiwara, M. B. Greenfield, M. N. Harakeh, T. Inomata, J. Jänecke, K. Katori, S. Nakayama, H. Sakai, Y. Sakemi, M. Tanaka, and M. Yosoi, *Phys. Rev. C* **52**, 604 (1995).
- [109] N. Paar, T. Nikšić, D. Vretenar, and P. Ring, *Phys. Rev. C* **69**, 054303 (2004).
- [110] J. Speth (ed.), *Electric and Magnetic Giant Resonances in Nuclei* (World Scientific, Singapore, 1991).
- [111] X. Roca-Maza, G. Colò, and H. Sagawa, *Phys. Rev. C* **86**, 031306(R) (2012).